Accepted Manuscript

Antibacterial evaluation of structurally amphipathic, membrane active small cationic peptidomimetics: Synthesized by incorporating 3-amino benzoic acid as peptidomimetic element

Sandeep Lohan, Swaranjit Singh Cameotra, Gopal Singh Bisht

PII: S0223-5234(14)00542-X

DOI: 10.1016/j.ejmech.2014.06.023

Reference: EJMECH 7066

To appear in: *European Journal of Medicinal Chemistry*

Received Date: 28 January 2014

Revised Date: 6 June 2014

Accepted Date: 12 June 2014

Please cite this article as: S. Lohan, S.S. Cameotra, G.S. Bisht, Antibacterial evaluation of structurally amphipathic, membrane active small cationic peptidomimetics: Synthesized by incorporating 3-amino benzoic acid as peptidomimetic element, *European Journal of Medicinal Chemistry* (2014), doi: 10.1016/j.ejmech.2014.06.023.

Newly designed small cationic peptidomimetics with potential antibacterial activity against antibiotic resistant pathogens (MRSA & MRSE)

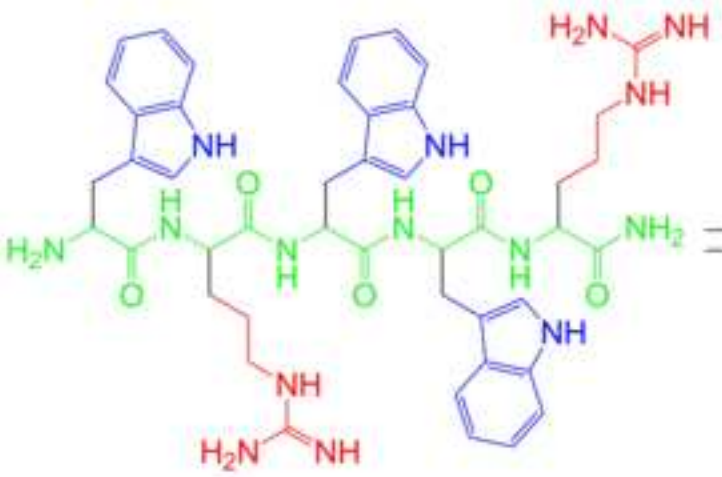

Linear peptide sequence (**5b**)

Structural transformation on the incorporation of

3-amino benzoic acid as peptidomimetic element

MIC (μg/mL)

Code	*S.aureus*	MRSA	MRSE
5b	15	17.5	20
4g	5	5.5	5

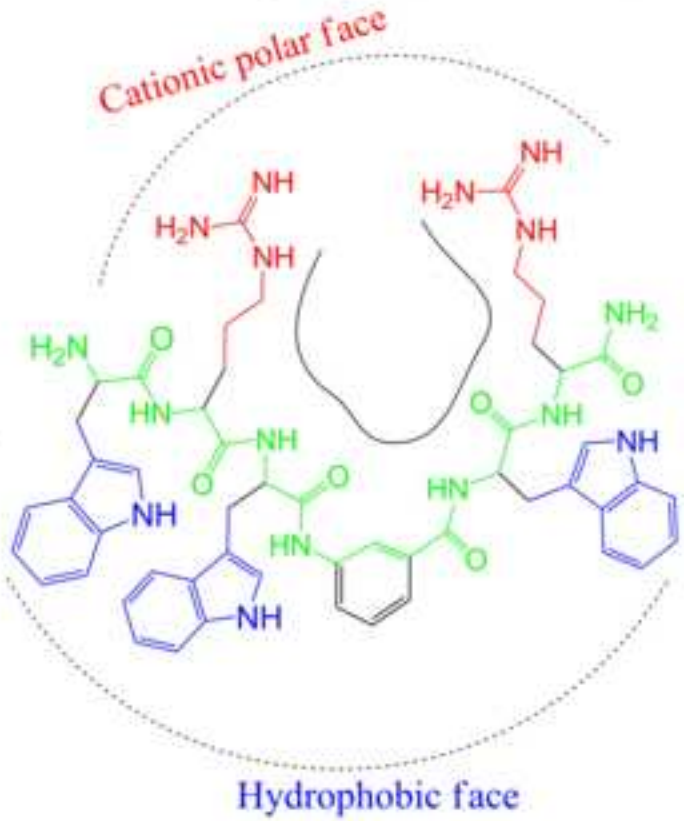

Peptidomimetic sequence (**4g**)

Highlights

- Synthesis of a series of 3-ABA based short cationic peptidomimetics.
- Lead peptidomimetics showed activity against MRSA & MRSE.
- Calcein dye leakage and fluorescent microscopy results display membrane disruption action on intact bacterial cells.
- Lead peptidomimetics were stable in plasma and even resistant pathogen (MRSA) was not able to develop resistance against them.

Antibacterial evaluation of structurally amphipathic, membrane active small cationic peptidomimetics: Synthesized by incorporating 3-amino benzoic acid as peptidomimetic element

Sandeep Lohan [a], Swaranjit Singh Cameotra [b], Gopal Singh Bisht [a]*

[a]*Department of Pharmacy, Jaypee University of Information Technology, Solan 173234, India.*

[b]*Environmental Biotechnology & Microbial Biochemistry, Institute of Microbial Technology, Chandigarh 160036, India.*

[*]**Corresponding Author:** Dr. Gopal Singh Bisht

Department of Pharmacy, Jaypee University of Information Technology, Solan, India.

Email: bishtchem2005@gmail.com

Tel: 91-1792-239336

Fax: +91-1792-245362

Abstract

A new series of small cationic peptidomimetics were synthesized by incorporating 3-amino benzoic acid (3-ABA) in a small structural framework with the objective to mimic essential properties of natural antimicrobial peptides (AMPs). The new design approach resulted into improvement of activity and selectivity in comparison to linear peptides and allowed us to better understand the influence of structural amphipathicity on biological activity. Lead peptidomimetics displayed antibacterial activities against resistant pathogens (MRSA & MRSE). A calcein dye leakage experiment revealed a membranolytic effect of **4g** and **4l** which was further confirmed by fluorescence microscopy. In addition, proteolytic stability and no sign of resistance development against *S. aureus* and MRSA demonstrate their potential for further development as novel antimicrobial therapeutics.

Keywords: Antibacterial peptidomimetics, 3-amino benzoic acid, Antibiotic resistance, Plasma stability.

1. Introduction

The near-explosive increased occurence in multi-drug resistant pathogens is recognized as a severe menace to public health in nations around the globe. Moreover, nowadays treatment options are becoming limited by the emergence of infections caused by pathogenic bacterial strains that are resistant to conventional antibiotics *viz* methicillin-resistant *Staphylococcus aureus* (MRSA), methicillin-resistant *Staphylococcus* epidermidis (MRSE), and vancomycin-resistant enterococci (VRE). Earlier, infections caused by multi-drug resistant bacterial strains were mostly limited to the nosocomial environment but community acquired resistant strains are now rising in prevalence [1-3]. There is an urgent need to develop classes of antibiotics with different mechanisms of action in comparison to existing antibiotics.

In the last decade, a number of studies were conducted to explore the potential of small cationic antimicrobial peptides (SCAMPs), designed by mimicking essential structural features of AMPs, as future antibiotics, especially because of their enzymatic stability and minimal propensity for resistance development [4-8]. AMPs are widespread in nature and have been isolated from virtually all multi-cellular organisms ranging from insects to humans. It has been well documented that these native peptide templates are vital components of innate immunity, as all forms of life use them as weapons to ward off pathogenic microbes in order to survive and thrive on this planet [9,10]. Although there is great structural diversity among AMPs, some common structural features which might be responsible for activity have been identified [11-13]. Structurally, native AMPs are quite large molecules ranging from 12 to 50 amino acid residues and adopt an amphipathic conformation in close proximity of biological membranes in such a way that hydrophobic and hydrophilic moieties segregates on opposite face of the molecular framework [14]. At physiological pH they usually possess a net positive charge (generally +2 to +9) due to the abundance of basic amino acids (lysine and arginine) in their sequence [15,16]. The cationic nature of these genes coded peptides drives them towards the negatively charged components

of bacterial cytoplasmic membrane that provides an initial mode of interaction. Further, the hydrophobic interactions between bulky side chains of AMPs and acyl tails of membrane phospholipids allow the peptides to penetrate the cell membrane [17,18]. The precise mechanism for lytic activity of AMPs is still a matter of debate, though several mechanisms have been proposed to describe the lipid-peptide interactions [19-23]. In addition, a number of AMPs are frequently referred as "host defense peptides" and have been found to initiate an adaptive immune system [10,24]. Apparently, AMPs with their non-specific modes of action might indeed decrease pathogens ability to develop resistance. Further, AMPs possess a broad antimicrobial activity spectrum against microbial strains resistant to the conventional antibiotics [9,25,26]. Thus, without any doubt, these attractive therapeutic features associated with AMPs underlines their candidature to develop them as today's antibiotics.

In an attempt to search novel antibacterial peptidomimetics, here we describe a novel series of small cationic peptidomimetics designed by incorporating 3-ABA in peptide sequences composed of 2 to 5 amino acid residues. As it is well known fact that the structural features of AMPs like the net content of charge and/or hydrophobic bulk and facial amphipathicity play a crucial role in their biological activity [12,13,27]. Consequently, to explore the structure-activity relationship of novel peptidomimetic templates we carried out the synthesis by varying sequence as well as a number of both cationic and hydrophobic amino acid residues. All peptidomimetic molecules were screened against Gram-positive and Gram-negative bacterial strains including MRSA and MRSE. In vitro toxicity has been assessed by measuring the lytic activity against human red blood cells. The bactericidal kinetic study of lead peptidomimetics was also performed. The interaction with bacterial membrane mimic liposomes has been used for an initial investigation of the bactericidal mechanism. The membrane perturbation effect of lead peptidomimetic molecules was further confirmed by fluorescent microscopy assay. To further assess the prospective of lead peptidomimetics as a

novel class of antibiotics, the proteolytic stability and potential of pathogen (susceptible as well as methicillin resistant *S. aureus*) to develop resistance against them was determined.

2. Results and discussion

2.1 Design and synthesis

Native AMPs and synthetically designed peptidomimetic templates comprised of genetically coded amino acid residues can be susceptible to proteolytic degradation [3-7]. Backbone modification is one of the synthetic approaches used to design peptidase immune peptidomimetics [6,7]. In addition, it is well documented that biological activity of native AMPs is depending on their secondary structure as well as net content of cationic charge and hydrophobicity [9,10]. Therefore, incorporation of any suitable moiety in the peptide backbone which provides a specific turn might improve stability and antimicrobial potential.

The aromatic γ-amino acid 3-ABA has a constrained structural framework due to the presence of two principal dihedral angles θ1 (C2-C3) and θ2 (C1-C2), sandwiched between φ (N-C3) and ψ (C1-CO). They have a fixed dihedral angle of about 180^{o}. Possibly, it may attribute to its β-sheet like structure (Figure 1) [28]. Rao *et al.* have incorporated 3-ABA in β-hairpin loop as turn inducing motif and shown that it result into very stable secondary structures [29]. Lundy *et al.* reported synthetic analogues of α-defensin (HNP-1) synthesized by incorporating constrained aromatic amino benzoic acids as β-turn motif exhibit broad-spectrum antibacterial activity [30]. Recently, Lengyel *et al.* reported that incorporation of 3-ABA in peptide sequence improved the stability of folded conformation in aqueous medium without effecting the arrangement of side chain residues [31]. Based on these observations, we hypothesize that the incorporation of constrained aromatic amino acid (3-ABA) could mimic essential structural features of AMPs in such a way that optimum therapeutic index may possibly be achieved.

Initially, a library of small cationic peptidomimetics (**1a, 2a-2c, 3a-3e, 4a-4g**) was synthesized by incorporating 3-amino benzoic acid (3-ABA) as peptidomimetic element

(Scheme 1). Arginine (Arg) and Tryptophan (Trp) amino acid residues were used to provide cationic charge and hydrophobic bulkiness respectively. We preferred arginine (Arg) over lysine because it behaves like charged moiety under all physiological conditions and also guanidine group would exhibit higher electrostatic interaction with the negatively charged phospholipids of bacterial cell membrane [8,32]. The selection of Trp was based on the presumption that the indole nucleus would be inserted into the membrane with the hydrophobic part interacting with the hydrophobic portion of the bilayer and the amine function interacting more closely with the polar head-groups of the membrane [33]. Strom *et al.* have previously documented that a specific content of both cationic charge and lipophilic bulk is required to design potent synthetic mimics of AMPs [8]. Consequently, peptidomimetic molecules were synthesized by varying the sequence of charged (Arg) and hydrophobic (Trp) amino acid residues on both sides of 3-ABA. Further peptidomimetic molecules (**3f** and **4h-4l**) were synthesized by replacing Arg with unnatural cationic amino acid ornithine (Orn) in the most active and moderately active molecules (**3e and 4c-4g)**. Structural modification was done by the substitution bulky hydrophobic residue Trp with Phe (**4m-4p**) among the most active molecules (**4f**, **4g, 4k** and **4l**). Finally, for comparative analysis, we synthesized linear peptide sequences (**5a-5d**) without incorporating 3-ABA.

2.2 Antibacterial activity

The activity results showed that peptidomimetic molecules were in general more potent against *S. aureus* and their resistant strains (MRSA & MRSE) than other bacterial strains (*B. subtilis*, *E. coli*, and *P. aeruginosa*) used in the study. These outcomes point out their predominant anti-staphylococcal behavior which is in agreement with previous reports [4,8]. Peptidomimetic molecules **1a, 2a-2c, 3a-3d** composed of 3, 4, and 5 amino acid residues, showed virtually no antibacterial activity. In some cases moderate activity was observed with the exception of the molecule **3e** that exhibited MIC values of 12.5, 10, and 12.5 µg/mL against *S. aureus*, MRSA, and MRSE respectively. The peptidomimetic molecule **3e** was also

active against *E. coli* and *P. aeruginosa*, although the MIC values were considerably higher in comparison to their activity against various strains of *S. aureus* (Table 1). Peptidomimetic molecules (**4a-4g**) with 6 amino acid residues displayed higher antibacterial activity against both Gram-positive and Gram-negative bacteria in comparison to peptidomimetic sequences with tri, tetra and penta amino acid residues. Most active peptidomimetic molecule **4g** displayed maximum potency with MIC values in the range of 5-5.5 µg/mL against *S. aureus*, MRSA, and MRSE. It was interesting to note that **4g** showed comparable activity against Gram-negative bacteria also with MIC values of 7.5 and 12.5 µg/mL against *E. coli* and *P. aeruginosa* respectively. Moreover, peptidomimetic molecule **4f** with 6 amino acid residues was found to be active against Gram-positive as well as Gram-negative bacteria. Same pattern of activity was observed in the case of **4l** which exhibited MIC values in the range of 5-6.25 µg/mL against *S. aureus*, MRSA, and MRSE. Peptidomimetic molecule **4l** was found to have somewhat low activity against Gram-negative bacteria with MICs 20 and 15.5 µg/mL against *E. coli* and *P. aeruginosa* respectively. The peptidomimetic molecules having phenylalanine as hydrophobic residue (**4m-4p**) showed insignificant lytic action against all screened bacterial strains. It was interesting to note that the linear peptide sequences without 3-ABA (**5a-5d**) showed poor antibacterial activity.

The activity results revealed a strong correlation between the antibacterial potency and overall structural amphipathicity of peptidomimetics. This can be illustrated by observing highest antibacterial activity in case of **4g** and **4l** which are having amphipathic structure. 3D view of the structural framework of lead peptidomimetics (**4g** and **4l)** and linear peptides (**5b** and **5d**) is shown in Figure 2. This structure-activity relationship was further confirmed by observing bacterial killing effect of **3e**, the only penta peptidomimetic having amphipathic structural framework. The presence of a hydrophobic structural motif composed of 3-ABA flanked by Trp residues is another common structural feature of active peptidomimetic molecules (**3e, 4f, 4g, 4k,** and **4l**; Figure 3). Wessolswski *et al.* have already reported that

small Arg-Trp rich AMPs with three adjacent aromatic residues display high bactericidal action [34]. In this way this could be another reason for the efficient antibacterial potency of newly designed peptidomimetics.

It was intresting to note that peptidomimetics **4f** and **4g** synthesized by incorporating 3-ABA displayed 3-4 fold of improvements in activity against *S. aureus*, MRSA, and MRSE in comparison to linear peptides **5a** and **5b**. In similar fashion, peptidomimetics having Orn as cationic residue (**4k** and **4l**) required nearly 8-10 fold of less concentration in comparison to linear peptides (**5c** and **5d**) to completely eradicate the growth of *S. aureus*, MRSA, and MRSE (Table 1). Therefore, the results demonstrated that this novel design principle may facilitate the development of new potent antibacterial peptidomimetics.

2.3 Hemolytic activity

We performed hemolytic assay by quantifying 50% (HC_{50}) as well as 10% hemolysis (HC_{10}) against human red blood cells (hRBCs) as a measurement of toxicity. In general, lengthy peptidomimetic derivatives (**4a-4p**) were found more hemolytic than smaller peptidomimetic derivatives (**1a**, **2a-2c**, and **3a-3f**) as summarized in Table 1. Thus, it seems that, as the hydrophobic bulk of peptidomimetic derivatives increases, their ability to discriminate between anionic bacterial surface and zwitterionic mammalian membrane decreases. These outcomes were in accordance with Kondejewski *et al*., who explored the correlation between hydrophobicity and hemolytic activity [35]. Maximum hemolysis determined by HC_{10} was detected for **4g** at 80 µg/mL. Other peptidomimetic sequences caused 10% hemolysis at a concentration above 100 µg/mL. Therefore, overall outcomes of hemolytic assay revealed that all synthesized peptidomimetics do not readily induce lysis of hRBCs. Furthermore, selectivity ratio (SR) was calculated by dividing HC_{50} values with the MICs against *S. aureus*. The maximum selectivity was observed for one of the lead peptidomimetic molecule **4l** (SR= 62.4) followed by **4g** (SR= 62; Table 1). In addition, the hemolytic activity results showed that our structural model increased the selectivity of peptidomimetic molecules as

lead peptidomimetics with 3-ABA scaffold (**4f**, **4g**, **4k**, and **4l**) displayed low hemolytic activity in comparison to linear peptides (**5a-5d**) as summarized in Table 1.

2.4. Cytotoxicity

The cytotoxicity of lead peptidomimetics (**4g** & **4l**) and linear peptides (**5b** & **5d**) was assessed by using MTT and LDH assays. The results of MTT assay showed that tested molecules (**4g**, **4l, 5b, and 5d**) caused a decrease in cell viability in a concentration dependent manner (Figure 4). However, **5b** and **5d** were found to be comparatively higher toxic toward HaCaT cells. Similarly, LDH assay results further revealed the lower toxicity of lead peptidomimetics (**4g** & **4l**) in comparison to linear peptides (**5b** & **5d**) (Figure 5). At each concentration level **5b** and **5d** induced higher levels of LDH release when compared with **4g** and **4l**.

2.5. Bactericidal kinetic assay

In comparison to the conventional antibiotics, AMPs are having fast bacterial killing kinetics [26,36]. To determine whether this ability is also inherent to newly designed peptidomimetics reported here, the viability of exponentially growing *S. aureus* and *E. coli* was checked against most potent peptidomimetics (**4g** and **4l**) by time-kill assay. Bactericidal kinetic study results demonstrated the rapid killing effect of lead peptidomimetics. Compound **4g** and **4l** at 4 × MIC decrease the number of *S. aureus* and *E. coli* from 10^6 CFU/mL to nearly10^3 CFU/mL with in 30 min (Figure 6A and 6B). The rapid bactericidal effect is usually observed among most of the membrane active AMPs. Thus, rapid bacterial killing effect of lead peptidomimetics (**4g** and **4l**) suggests that their antibacterial action might be mediated through permeabilization of the bacterial membrane.

2.6. Calcein dye leakage

Membrane disruption is generally considered as the plausible mode of action for most of the naturally occurring AMPs and synthetically designed small cationic antimicrobial peptidomimetics [25,37,38]. In order to assess membrane interaction behavior of **4g** and **4l**,

we performed calcein dye leakage experiment by designing negatively charged and zwitterionic calcein encapsulated liposomes which mimics the outer surface of bacterial and mammalian cell membranes respectively. Fluorescent dye leakage experiment results showed that **4g** induces dye leakage in a concentration dependent manner, as 47% of dye was released at a highest experimental concentration (15 µg/mL) after approx. 20 min and 19% dye was released at lowest concentration (5 µg/mL) after nearly 50 min. In an analogous manner to **4g**, **4l** also induces dye leakage in a dose dependent manner as 23% leakage was observed after 90 min at 5 µg/mL that increased to 48% at a concentration of 15 µg/mL after the same time interval (Figure 7). While in case of mammalian membrane mimic liposomes negligible amount of dye leakage was observed even at maximum used experimental concentration (15 µg/mL) of both **4g** and **4l**. Therefore, results of dye leakage experiment support the activity results as **4g** exhibits higher MIC values against all tested strains of bacteria in comparison to **4l**. The calcein dye leakage experiment indicated that, the biological activity of these peptidomimetics is dependent on their ability to permeate target membranes, same as that of AMPs.

2.7. Fluorescence Microscopy

To further investigate the mechanism involved in antibacterial activity of newly designed peptidomimetics, the ability of two most potent sequences **4g** and **4l** to cause membrane damage was assessed by fluorescence microscopy (Figure 8). The effect of active sequences on both Gram-negative (*E. coli*) and Gram-positive (*S. aureus*) bacteria were studied by a double staining method with DAPI (4’,6-diamidino-2-phenylindole) and PI (propidium iodide). In the first step bacterial strains (*E. coli* and *S. aureus*) were incubated with **4g** and **4l** for 2 h after that cells were stained with DAPI, which stains all bacterial cells in blue irrespective of their viability and PI, which penetrates only injured or dead cells with compromised membranes. In control (without initial treatment with peptidomimetics), both *E. coli* and *S. aureus* showed blue fluorescence with DAPI, while negligible number of cells

had red fluorescence with PI. On the other hand, in case of treated *E. coli* and *S. aureus* cells, stronger red fluorescence was observed with PI (Figure 8). Comparatively intense red fluorescence was observed for *S. aureus*, suggesting their significant membrane damage, which fully supports our activity results. These results collectively indicate that **4g** and **4I** effectively arrest bacterial growth, via a membrane disruption mechanism similar to most of the native AMPs.

2.8. Resistance study

The efficacy of conventionally used antibiotics in treating infections caused by drug resistant pathogens has been diminished as a result of pathogens ability to switch on to an alternate metabolic pathway. It has already been reported that low propensity of resistance development was observed in case of therapeutics that kill bacteria by targeting cell membrane [25,39]. Therefore, we have determined the potential of susceptible pathogenic *S. aureus* as well as MRSA, a clinically relevant drug resistant bacteria pathogen, to develop drug resistance against most potent sequences **4g** and **4l**. The new MIC values were determined every 24 h after propagation of bacterial cultures with fresh media and serially diluted concentrations of tested peptidomimetics. To make comparative analysis, parallel cultures were exposed to 2-fold dilutions of the antibiotic ciprofloxacin as a positive control. The experiment was repeated for 16 days. Results in figure 9 show the low propensity of bacterial pathogens to develop resistance against **4g** and **4l** as there was almost no change in the MIC after 16 passages.

2.9. Plasma stability study

Most of the naturally occurring AMPs are fairly large molecules, and therefore are having number of scissile amide bonds in their structural framework that can be easily targeted by proteolytic enzymes [6,7]. The inherent instability of these potent antimicrobial templates renders them considerably inactive in intended bioenvironment. Therefore, this is an issue that needs to be resolved for commercialization of these promising compounds. In this

respect, to assess the biocompatibility of lead peptidomimetics **4g** and **4l**, we conducted their stability study in human blood plasma. **4g** was not degraded when incubated in plasma for 1 h and minute degradation (6.58%) was observed after 2 h incubation in plasma. It was interesting to note that further degradation of **4g** did not take place even after 24 h incubation in plasma as no extra peak was observed (see Supporting Information; Figure S1). On the other hand, no sign of degradation was detected for **4l** even after 24 h incubation in plasma (Figure S2). This is may be due to the presence of non genitically coded amino acid Orn, which is not a well known substrate for proteolytic enzymes.

To determine the effectiveness of our novel synthetic approach regarding proteolytic stability we also carried out the plasma stability study of linear peptides (**5b** & **5d**). Minute degradation (5.31%) of **5b** was detected after 30 min incubation and it was further increased (11.79%) when incubated for 1 h in plasma. No more enzymatic degradation of **5b** was takes place when incubated in plasma for 12 h and 18% of **5b** was degraded when incubated in plasma for 24 h (Figure S3). Small amount of enzymatic degradation (4.72%) was detected for **5d** after 30 min incubation in plasma and it was no more degraded when incubated in plasma for 24 h (Figure S4). The outcomes of stability study revealed that incorporation of 3-ABA enhanced the stability against proteolytic enzymes as **4g** and **4l** were found to be higher stable in plasma in comparison to linear peptides **5b** and **5d**.

2.10. Proteolytic stability

To further ensure the proteolytic stability of lead peptidomimetics, we carried out trypsin and α-chemotrypsin digestion assay. The results from the stability study on peptidomimetics (**4g** and **4l**) and linear peptides (**5b** and **5d**) were rather striking. **4g** was found stable against trypsin when incubated for 36 h and after that it was slowly degraded with approximately 65% of the peptidomimetic remaining after 4 days (Figure 10A). However, linear peptide sequence (**5b**) showed higher susceptibility towards trypsin as only 21% of the peptide remaining after 4 days. Noticeably, a negligible amount of tryptic degradation was observed

for **4l**. In addition, linear peptide **5d** also showed good stability with nearly 82% of the parent peptide remaning after 4 days. It is well documented that trypsin cleaves C-terminal to native cationic amino acids such as Lys and Arg [6]. Thus, the presence of non-natural cationic amino acid Orn might be responsible for the high stability of **4l** and **5d** against tryptic degradation. Furthermore, the high stability of **4g** and **4l** as compared to **5b** and **5d** respectively, showed that 3-ABA may be a valuable building block by protecting scissile peptide bonds against tryptic degradation. Peptidomimetics **4g** and **4l** were seemingly completely stable against proteolytic degradation by α-chemotrypsin for 24 h, and after that slow degradation was observed with nearly 70% of the peptidomimetics were still intact after 4 days (Figure 10B). On the other hand, linear peptides (**5b** and **5d**) were gradually degraded when incubated with α-chemotrypsin and only 44% of the intact peptides remaining after 4 days. Mechanistically, α-chymotrypsin cleaves the peptide bond on the C-terminal side of bulky hydrophobic amino acids (Phe, Trp) [7]. Accordingly, the better stability of **4g** and **4l** against α-chymotrypsin might be due to the presence of 3-ABA. The results, thereby collectively demonstrated that the incorporation of Orn as well as 3-ABA could render the peptide sequences immune against proteolytic enzymes.

3. Conclusions

In conclusion, our novel structural model has resulted in the identification of potent antibacterial peptidomimetics that exhibit higher activity as compared to peptide sequences without 3-ABA. In addition, newly designed peptidomimetic templates show specificity toward bacteria relative to eukaryotic red blood cells. Based on the results of calcein leakage experiment and fluorescent microscopic data on lead peptidomimetics **4g** and **4l**, we propose that they are more prone to membrane damage mode of action which is similar to most of the native AMPs. The lead compounds **4g** and **4l** display other essential properties such as improved proteolytic stability and insignificant capability of pathogens to develop resistance

against them. Thus, the lead obtained from present study could be optimized for therapeutic use against drug resistant bacterial strains.

4. Experimental Section

4.1. Chemicals and reagents

Rink amide MBHA resin and protected amino acids Fmoc-Arg(pbf)-OH, Fmoc-Trp(Boc)-OH, Fmoc-Phe-OH and Fmoc-Orn(Boc)-OH were purchased from Novabiochem (Mumbai, India). Aromatic amino acid 3-amino benzoic acid and Fmoc-Cl were obtained from Spectrochem (Mumbai, India). Other reagents used for solid phase synthesis of peptidomimetic molecules included N-hydroxybenzotrizole (HOBt), N,N'-diisopropylcarbodiimide (DIC), Piperidine, N,N-dimethylformamide (DMF) (Spectrochem, Mumbai, India), dimethylsulphoxide (DMSO), dichloromethane (DCM), 1,2-Ethanedithiol (Merck, Mumbai, India), and Trifluoro acetic acid (TFA; Loba chemie, Mumbai, India). Membrane bilayers mimic phospholipids dipalmitoylphosphatidylcholine (DPPC) and dipalmitoylphosphatidylglycerol (DPPG) were purchased from Avanti Polar Lipids (New Delhi, India). Calcein, propidium iodide, DAPI and buffer material were purchased from Sigma-Aldrich (India). Dulbecco's modified Eagle's medium (DMEM), 3-(4,5-dimethylthiazol-2-yl)-2,5-diphenyltetrazolium bromide (MTT), were obtained from Sigma Chemical Co. (St Louis, MO, USA). The lactate dehydrogenase (LDH) assay kit was purchased from Promega (Madison, WI, USA). All the solvents used for purification were of HPLC grade and obtained from Merck (Mumbai, India). Buffers were prepared in double-distilled water.

4.2. General procedure for the Fmoc protection of 3-amino benzoic acid

To a solution of 3-amino benzoic acid (1.37 g, 10 mmol) in water (35 mL), was added sodium hydrogen carbonate (2.52 g, 30 mmol), and the resulting mixture was cooled to 5 °C and it was slowly added with Fmoc-Cl (3.87 g, 15 mmol) as a solution in *para*-dioxane. The resulting mixture was stirred at 0 °C for 1 h and allowed to warm to room temperature

overnight. Completion of the reaction was monitored by precoated TLC plate. After the completion of reaction water was added to the reaction mixture and the aqueous layer was extracted with ethyl acetate. Then the organic layer was extracted twice with a saturated aqueous solution of sodium bicarbonate. The combined aqueous layers were acidified to a pH of 2 with 10% HCl, and then extracted three times with ethyl acetate. The combined organic layers were removed under reduced pressure to isolate the title compound. The crude material was used without any further purification.

4.2.1. Fmoc-3-ABA: ^{1}H NMR (400 MHz, DMSO d_6) δ: 12.21 (s, 1H), 9.81 (s, 1H), 7.91 - 7.66 (m, 6H), 7.52 - 7.27 (m, 6H), 4.47 - 4.45 (d, J = 8Hz, 2H), 4.26 - 4.23 (t, J = 12Hz, 1H). MALDI-TOF: calcd for $C_{22}H_{17}NO_4$: 359.12, found 360.39.

4.3. General procedure for solid phase synthesis of peptidomimetics

All peptidomimetics were synthesized manually following standard Fmoc solid phase protocols using Rink amide-4-methylbenzhydrylamine hydrochloride salt (MBHA) resin (loading 0.79 mmol/g) as solid support [40]. Rink amide resin (150 mg) was washed with CH_2Cl_2 (3 × 2 mL), which is followed by swelling in DMF (3.5 mL) for 25 min. The Fmoc protecting group of resin was removed by treating with piperidine/DMF (20% v/v) mixture for 10 min, followed by extensive washes with DMF (5 × 2 mL). The deprotection step was performed twice. Each amino acid coupling step included an Fmoc deprotection and 3 h coupling of 4 equiv of Fmoc protected amino acid onto resin in the presence 2 equiv of DIC/HOBt in DMF. After the desired sequences were assembled, the peptidomimetic molecules were cleaved with a solution of TFA/H_2O/1,2-Ethanedithiol (95:2.5:2.5) from solid support (Scheme 1).

4.4. Purification

All crude peptidomimetics were analysed on a reversed-phase high performance liquid chromatography (RP-HPLC) using a C_{18} waters column (Spherisorb®, ODS2, 5µm, 4.6 mm × 250 mm) at room temperature. A linear gradient of 0.5-60% solvent B (0.05% TFA in

acetonitrile) in solvent A (0.05% TFA in water) over 35 min, followed by 60-0.5% solvent B over 10 min was used at a flow rate of 0.5 mL/min. Preparative RP-HPLC was then performed on a Waters column (Spherisorb® , ODS2, 5µm, 20 mm × 250 mm) using 0.5-60% linear gradient of solvent B (0.05% TFA in acetonitrile) in solvent A (0.05% TFA in water) over 35 min, followed by 60-0.5% solvent B over 10 min at a flow rate of 5 mL/min. Mass spectra were obtained on a Agilent MALDI-TOF mass spectrometer. Purified HPLC fractions were than lyophilized. See the supporting information for analytical data (Mass spectra, ^{1}H NMR, and HPLC chromatograms).

4.4.1. H-Trp-3ABA-Arg-NH$_2$ **(1a):** ^{1}H NMR (400 MHz, DMSO d_6) δ: 10.98 (s, 1H), 10.91 (s, 2H), 10. 80 (s, 1H), 10.76 (s, 2H), 9.42 (s, 2H), 8.80 (s, 1H), 8.16 - 8.15 (d, *J* = 4Hz, 2H), 7.33 - 6.97 (m, 8H), 4.67 - 4.64 (t, *J* = 12Hz, 1H), 4.22 - 4.19 (t, *J* = 12Hz, 1H), 3.19 - 3.18 (d, *J* = 4Hz, 5H), 2.84 (s, 1H), 2.46 - 2.45 (t, *J* = 4Hz, 3H), 1.25 - 1.22 (m, 2H), 1.12 - 1.11 (m, 2H). MALDI-TOF: calcd for $C_{24}H_{30}N_8O_3$: 478.24, found 479.24; Purity determined by RP-HPLC: Retention time: 26.55 min, purity: 97.61%.

4.4.2. H-Trp-Trp-3ABA-Arg-NH$_2$ **(2a):** ^{1}H NMR (400 MHz, DMSO d_6) δ: 11.19 (s, 2H), 10.90 (s, 1H), 10.82 (s, 1H), 10. 76 (s, 2H), 10.34 (s, 2H), 9.37 (s, 1H), 8.63 (s, 2H), 7.90 - 7.89 (d, *J* = 4Hz, 2H), 7.30 - 6.97 (m, 12H), 4.67 - 4.65 (m, 2H), 4.39 - 4.38 (t, *J* = 4Hz, 1H), 3.19 - 3.18 (d, *J* = 4Hz, 5H), 2.84 (s, 1H), 2.47 - 2.45 (m, 3H), 1.25 - 1.11 (m, 4H). MALDI-TOF: calcd for $C_{35}H_{40}N_{10}O_4$: 664.32, found 665.12; Purity determined by RP-HPLC: Retention time: 28.66 min, purity: 98.62%.

4.4.3. H-Arg-Trp-3ABA-Arg-NH$_2$ **(2b):** ^{1}H NMR (400 MHz, DMSO d_6) δ: 11.12 (s, 1H), 10.86 (s, 2H), 10.80 (s, 2H), 10. 32 (s, 1H), 10.14 (s, 2H), 9.19 (s, 2H), 8.44 (s, 2H), 7.93 - 7.91 (d, *J* = 8Hz, 2H), 7.31 - 7.01 (m, 7H), 4.62 - 4.57 (m, 2H), 4.37 - 4.35 (t, *J* = 8Hz, 1H), 3.21 - 3.20 (d, *J* = 4Hz, 2H), 2.81 (s, 2H), 2.43 - 2.40 (m, 4H), 1.27 - 1.12 (m, 8H). MALDI-TOF: calcd for $C_{30}H_{42}N_{12}O_4$: 634.35, found 635.44; Purity determined by RP-HPLC: Retention time: 23.82 min, purity: 98.77%.

4.4.4. H-Trp-Arg-3ABA-Arg-NH$_2$ **(2c):** ^{1}H NMR (400 MHz, DMSO d_6) δ: 11.09 (s, 1H), 10.81 (s, 2H), 10.79 (s, 2H), 10. 41 (s, 1H), 10.02 (s, 2H), 8.97 (s, 2H), 8.29 (s, 2H), 7.87 - 7.85 (d, *J* = 8Hz, 2H), 7.35 - 7.07 (m, 7H), 4.71 - 4.66 (m, 2H), 4.32 - 4.31 (t, *J* = 4Hz, 1H), 3.19 - 3.17 (d, *J* = 8Hz, 2H), 2.81 (s, 2H), 2.49 - 2.45 (m, 4H), 1.28 - 1.14 (m, 8H). MALDI-TOF: calcd for $C_{30}H_{42}N_{12}O_4$: 634.35, found 635.39; Purity determined by RP-HPLC: Retention time: 24.18 min, purity: 97.34%.

4.4.5. H-Trp-Trp-3ABA-Arg-Arg-NH$_2$ **(3a):** ^{1}H NMR (400 MHz, DMSO d_6) δ: 11.14 (s, 2H), 10.80 (s, 2H), 10.76 (s, 2H), 10. 29 (s, 2H), 9.91 (s, 4H), 8.90 (s, 2H), 8.22 (s, 2H), 7.74 - 7.71 (d, *J* = 12Hz, 2H), 7.29 - 6.98 (m, 12H), 4.82 - 4.77 (m, 3H), 4.30 - 4.29 (t, *J* = 4Hz, 1H), 3.18 - 3.16 (d, *J* = 8Hz, 4H), 2.80 (s, 2H), 2.51 - 2.46 (m, 4H), 1.29 - 1.13 (m, 8H). MALDI-TOF: calcd for $C_{41}H_{52}N_{14}O_5$: 820.42, found 821.19; Purity determined by RP-HPLC: Retention time: 25.37 min, purity: 95.66%.

4.4.6. H-Arg-Trp-3ABA-Arg-Arg-NH$_2$ **(3b):** ^{1}H NMR (400 MHz, DMSO d_6) δ: 11.04 (s, 1H), 10.78 (s, 6H), 10.71 (s, 2H), 10. 27 (s, 2H), 9.93 (s, 4H), 8.88 (s, 3H), 8.20 (s, 2H), 7.71 - 7.69 (d, *J* = 8Hz, 2H), 7.28 - 7.09 (m, 8H), 4.80 - 4.74 (m, 3H), 4.29 - 4.27 (t, *J* = 8Hz, 1H), 3.16 - 3.15 (d, *J* = 4Hz, 2H), 2.81 (s, 3H), 2.50 - 2.43 (m, 6H), 1.26 - 1.11 (m, 13H). MALDI-TOF: calcd for $C_{36}H_{54}N_{16}O_5$: 790.45, found 791.44; Purity determined by RP-HPLC: Retention time: 22.534 min, purity: 95.67%.

4.4.7. H-Trp-Arg-3ABA-Arg-Arg-NH$_2$ **(3c):** ^{1}H NMR (400 MHz, DMSO d_6) δ: 11.07 (s, 1H), 10.81 (s, 6H), 10.70 (s, 2H), 10. 29 (s, 2H), 9.71 (s, 4H), 8.81 (s, 3H), 8.25 (s, 2H), 7.71 - 7.69 (d, *J* = 8Hz, 2H), 7.31 - 7.11 (m, 8H), 4.82 - 4.74 (m, 3H), 4.30 - 4.27 (t, *J* = 12Hz, 1H), 3.18 - 3.16 (d, *J* = 8Hz, 2H), 2.83 (s, 3H), 2.51 - 2.46 (m, 6H), 1.21 - 1.10 (m, 13H). MALDI-TOF: calcd for $C_{36}H_{54}N_{16}O_5$: 790.45, found 791.41; Purity determined by RP-HPLC: Retention time: 22.640 min, purity: 98.38%.

4.4.8. H-Trp-Arg-3ABA-Trp-Arg-NH$_2$ **(3d):** ^{1}H NMR (400 MHz, DMSO d_6) δ: 11.10 (s, 2H), 10.87 (s, 2H), 10.70 (s, 2H), 10. 12 (s, 2H), 9.84 (s, 4H), 8.79 (s, 2H), 8.23 (s, 2H), 7.65 -

7.63 (d, *J* = 8Hz, 2H), 7.36 - 7.02 (m, 13H), 4.79 - 4.73 (m, 3H), 4.29 - 4.27 (t, *J* = 8Hz, 1H), 3.20 - 3.17 (d, *J* = 12Hz, 5H), 2.84 (s, 2H), 2.53 - 2.44 (m, 4H), 1.26 - 1.11 (m, 9H). MALDI-TOF: calcd for $C_{41}H_{52}N_{14}O_5$: 820.42, found 821.33; Purity determined by RP-HPLC: Retention time: 24.98 min, purity: 96.14%.

4.4.9. H-Arg-Trp-3ABA-Trp-Arg-NH₂ **(3e):** ^{1}H NMR (400 MHz, DMSO d_6) δ: 11.12 (s, 2H), 10.81 (s, 2H), 10.78 (s, 2H), 10. 23 (s, 2H), 9.86 (s, 4H), 8.94 (s, 2H), 8.19 (s, 2H), 7.72 - 7.70 (d, *J* = 8Hz, 2H), 7.33 - 6.99 (m, 14H), 4.86 - 4.81 (m, 3H), 4.33 - 4.31 (t, *J* = 8Hz, 1H), 3.20 - 3.18 (d, *J* = 8Hz, 4H), 2.84 (s, 2H), 2.56 - 2.49 (m, 4H), 1.27 - 1.13 (m, 8H). MALDI-TOF: calcd for $C_{41}H_{52}N_{14}O_5$: 820.42, found 821.41; Purity determined by RP-HPLC: Retention time: 23.89 min, purity: 98.17%.

4.4.10. H-Trp-Trp-Arg-3ABA-Arg-Arg-NH₂ **(4a):** ^{1}H NMR (400 MHz, DMSO d_6) δ: 10.96 (s, 1H), 10.90 (s, 3H), 10.82 (s, 2H), 10. 76 (s, 4H), 10.35 (s, 2H), 9.37 (s, 6H), 8.51 (s, 2H), 7.94 - 7.93 (d, *J* = 4Hz, 2H), 7.75 - 7.57 (m, 4H), 7.48 - 6.96 (m, 8H), 4.70 - 4.65 (m, 3H), 4.21 - 4.19 (t, *J* = 8Hz, 2H), 3.14 - 3.12 (d, *J* = 8Hz, 8H), 2.83 (s, 3H), 2.47 - 2.45 (m, 6H), 1.24 - 1.08 (m, 14H). MALDI-TOF: calcd for $C_{47}H_{64}N_{18}O_6$: 976.53, found 977.23; Purity determined by RP-HPLC: Retention time: 27.340 min, purity: 98.42%.

4.4.11. H-Arg-Trp-Arg-3ABA-Trp-Arg-NH₂ **(4b):** ^{1}H NMR (400 MHz, DMSO d_6) δ: 10.98 (s, 1H), 10.88 (s, 3H), 10.80 (s, 2H), 10. 77 (s, 4H), 10.32 (s, 2H), 9.34 (s, 6H), 8.52 (s, 2H), 7.95 - 7.94 (d, *J* = 4Hz, 2H), 7.71 - 7.53 (m, 4H), 7.44 - 6.90 (m, 8H), 4.68 - 4.61 (m, 3H), 4.24 - 4.22 (t, *J* = 8Hz, 2H), 3.13 - 3.11 (d, *J* = 8Hz, 8H), 2.84 (s, 3H), 2.47 - 2.44 (m, 6H), 1.25 - 1.07 (m, 14H). MALDI-TOF: calcd for $C_{47}H_{64}N_{18}O_6$: 976.53, found 977.29; Purity determined by RP-HPLC: Retention time: 27.446 min, purity: 98.07%.

4.4.12. H-Arg-Trp-Trp-3ABA-Arg-Arg-NH₂ **(4c):** ^{1}H NMR (400 MHz, DMSO d_6) δ: 10.98 (s, 1H), 10.89 (s, 3H), 10.81 (s, 2H), 10. 76 (s, 4H), 10.36 (s, 2H), 9.39 (s, 6H), 8.52 (s, 2H), 7.96 - 7.93 (d, *J* = 12Hz, 2H), 7.71 - 7.58 (m, 4H), 7.44 - 6.91 (m, 8H), 4.69 - 4.64 (m, 3H), 4.22 - 4.20 (t, *J* = 8Hz, 2H), 3.13 - 3.11 (d, *J* = 8Hz, 8H), 2.82 (s, 3H), 2.46 - 2.43 (m, 6H),

1.25 - 1.08 (m, 14H). MALDI-TOF: calcd for $C_{47}H_{64}N_{18}O_6$: 976.53, found 977.19; Purity determined by RP-HPLC: Retention time: 26.960 min, purity: 96.61%.

4.4.13. H-Trp-Arg-Arg-3ABA-Trp-Arg-NH_2 **(4d):** ^{1}H NMR (400 MHz, DMSO d_6) δ: 10.97 (s, 1H), 10.89 (s, 3H), 10.82 (s, 2H), 10. 76 (s, 4H), 10.35 (s, 2H), 9.39 (s, 6H), 8.52 (s, 2H), 7.95 - 7.93 (d, *J* = 8Hz, 2H), 7.72 - 7.54 (m, 4H), 7.40 - 6.90 (m, 8H), 4.70 - 4.64 (m, 3H), 4.22 - 4.20 (t, *J* = 8Hz, 2H), 3.13 - 3.12 (d, *J* = 4Hz, 8H), 2.84 (s, 3H), 2.47 - 2.45 (m, 6H), 1.24 - 1.08 (m, 14H). MALDI-TOF: calcd for $C_{47}H_{64}N_{18}O_6$: 976.53, found 977.27; Purity determined by RP-HPLC: Retention time: 27.660 min, purity: 97.46%.

4.4.14. H-Trp-Arg-Trp-3ABA-Arg-Arg-NH_2 **(4e):** ^{1}H NMR (400 MHz, DMSO d_6) δ: 10.98 (s, 1H), 10.89 (s, 3H), 10.81 (s, 2H), 10. 76 (s, 4H), 10.36 (s, 2H), 9.42 (s, 6H), 8.55 (s, 2H), 7.95 - 7.94 (d, *J* = 4Hz, 2H), 7.72 - 7.54 (m, 4H), 7.43 - 6.91 (m, 8H), 4.70 - 4.64 (m, 3H), 4.22 - 4.20 (t, *J* = 8Hz, 2H), 3.13 - 3.11 (d, *J* = 8Hz, 8H), 2.84 (s, 3H), 2.48 - 2.45 (m, 6H), 1.25 - 1.08 (m, 14H). MALDI-TOF: calcd for $C_{47}H_{64}N_{18}O_6$: 976.53, found 977.53; Purity determined by RP-HPLC: Retention time: 27.324 min, purity: 96.06 %.

4.4.15. H-Arg-Arg-Trp-3ABA-Trp-Arg-NH_2 **(4f):** ^{1}H NMR (400 MHz, DMSO d_6) δ: 10.98 (s, 1H), 10.89 (s, 3H), 10.80 (s, 2H), 10. 76 (s, 4H), 10.36 (s, 2H), 9.39 (s, 6H), 8.52 (s, 2H), 7.95 - 7.93 (d, *J* = 8Hz, 2H), 7.72 - 7.58 (m, 4H), 7.44 - 6.91 (m, 8H), 4.70 - 4.64 (m, 3H), 4.22 - 4.19 (t, *J* = 12Hz, 2H), 3.13 - 3.12 (d, *J* = 4Hz, 8H), 2.84 (s, 3H), 2.47 - 2.45 (m, 6H), 1.25 - 1.08 (m, 14H). MALDI-TOF: calcd for $C_{47}H_{64}N_{18}O_6$: 976.53, found 977.39; Purity determined by RP-HPLC: Retention time: 27.402 min, purity: 99.65%.

4.4.16. H-Trp-Arg-Trp-3ABA-Trp-Arg-NH_2 **(4g):** ^{1}H NMR (400 MHz, DMSO d_6) δ: 10.98 (s, 3H), 10.91 (s, 2H), 10.80 (s, 1H), 10. 76 (s, 4H), 10.36 (s, 3H), 9.31 (s, 5H), 8.51 (s, 2H), 8.16 - 8.15 (d, *J* = 8Hz, 2H), 7.74 - 7.56 (m, 8H), 7.44 - 6.84 (m, 9H), 4.70 - 4.62 (m, 2H), 4.22 - 4.19 (t, *J* = 8Hz, 3H), 3.24 - 3.22 (d, *J* = 8Hz, 8H), 2.84 (s, 2H), 2.47 - 2.45 (m, 4H), 1.25 - 1.22 (m, 4H), 1.13 - 1.07 (m, 4H). MALDI-TOF: calcd for $C_{52}H_{62}N_{16}O_6$: 1006.5, found 1007.49; Purity determined by RP-HPLC: Retention time: 29.754 min, purity: 98.42%.

4.4.17. H-Orn-Trp-3ABA-Trp-Orn-NH$_2$ **(3f):** ^{1}H NMR (400 MHz, DMSO d_6) δ: 10.91 (s, 2H), 10.83 (s, 2H), 10.80 (s, 1H), 10. 21 (s, 2H), 9.50 (s, 3H), 8.54 (s, 4H), 8.14 - 8.12 (d, *J* = 8Hz, 2H), 7.83 - 7.44 (m, 12H), 4.67 - 4.58 (m, 3H), 4.23 - 4.21 (t, *J* = 8Hz, 1H), 3.32 - 3.28 (d, *J* = 16Hz, 5H), 2.49 - 2.44 (m, 5H), 1.72 - 1.61 (m, 4H), 1.26 - 1.08 (m, 4H). MALDI-TOF: calcd for $C_{39}H_{48}N_{10}O_5$: 736.38, found 737.18; Purity determined by RP-HPLC: Retention time: 24.231 min, purity: 98.74%.

4.4.18. H-Orn-Trp-Trp-3ABA-Orn-Orn-NH$_2$ **(4h):** ^{1}H NMR (400 MHz, DMSO d_6) δ: 10.97 (s, 2H), 10.85 (s, 2H), 10.78 (s, 2H), 10. 38 (s, 2H), 9.54 (s, 3H), 8.81 (s, 6H), 8.61 - 8.58 (d, *J* = 12Hz, 2H), 8.51 - 8.42 (m, 4H), 8.35 - 7.88 (m, 4H), 7.49 - 6.99 (m, 5H), 4.70 - 4.61 (m, 3H), 4.34 - 4.20 (m, 2H), 3.27 - 3.23 (d, *J* = 16Hz, 5H), 2.83 - 2.68 (m, 5H), 2.47 - 2.45 (m, 2H), 1.72 - 1.55(m, 7H), 1.27 - 1.07 (m, 6H). MALDI-TOF: calcd for $C_{44}H_{58}N_{12}O_6$: 850.46, found 851.47; Purity determined by RP-HPLC: Retention time: 23.979 min, purity: 96.31%.

4.4.19. H-Trp-Orn-Orn-3ABA-Trp-Orn-NH$_2$ **(4i):** ^{1}H NMR (400 MHz, DMSO d_6) δ: 10.98 (s, 2H), 10.84 (s, 1H), 10.81 (s, 2H), 10. 38 (s, 2H), 9.50 (s, 4H), 8.79 (s, 6H), 8.66 - 8.63 (d, *J* = 12Hz, 2H), 8.51 - 8.43 (m, 5H), 8.35 - 7.83 (m, 4H), 7.46 - 6.90 (m, 6H), 4.68 - 4.61 (m, 3H), 4.37 - 4.24 (m, 2H), 3.52 - 3.47 (d, *J* = 20Hz, 5H), 2.83 - 266 (m, 6H), 2.47 - 2.45 (m, 2H), 1.72 - 1.54 (m, 7H), 1.25 - 1.08 (m, 6H). MALDI-TOF: calcd for $C_{44}H_{58}N_{12}O_6$: 850.46, found 851.37; Purity determined by RP-HPLC: Retention time: 24.193 min, purity: 98.57%.

4.4.20. H-Trp-Orn-Trp-3ABA-Orn-Orn-NH$_2$ **(4j):** ^{1}H NMR (400 MHz, DMSO d_6) δ: 10.98 (s, 2H), 10.85 (s, 1H), 10.80 (s, 2H), 10. 41 (s, 2H), 9.52 (s, 4H), 8.79 (s, 6H), 8.64 - 8.61 (d, *J* = 12Hz, 2H), 8.47 - 8.39 (m, 5H), 8.33 - 7.80 (m, 4H), 7.45 - 6.88 (m, 6H), 4.70 - 4.58 (m, 3H), 4.38 - 4.24 (m, 2H), 3.67 - 3.62 (d, *J* = 20Hz, 5H), 2.81 - 265 (m, 6H), 2.46 - 2.45 (m, 2H), 1.71 - 1.54 (m, 7H), 1.26 - 1.07 (m, 6H). MALDI-TOF: calcd for $C_{44}H_{58}N_{12}O_6$: 850.46, found 851.41; Purity determined by RP-HPLC: Retention time: 24.782 min, purity: 98.38%.

4.4.21. H-Orn-Orn-Trp-3ABA-Trp-Orn-NH$_2$ **(4k):** ^{1}H NMR (400 MHz, DMSO d_6) δ: 10.98 (s, 2H), 10.85 (s, 1H), 10.81 (s, 1H), 10. 38 (s, 2H), 9.50 (s, 5H), 8.79 (s, 6H), 8.64 - 8.62 (d,

J = 8Hz, 2H), 8.49 - 8.42 (m, 5H), 8.34 - 7.83 (m, 4H), 7.46 - 6.90 (m, 6H), 4.69 - 4.61 (m, 3H), 4.37 - 4.21 (m, 2H), 3.68 - 3.60 (d, *J* = 32Hz, 5H), 2.84 - 266 (m, 6H), 2.47 - 2.45 (m, 2H), 1.72 - 1.54 (m, 7H), 1.25 - 1.07 (m, 6H). MALDI-TOF: calcd for $C_{44}H_{58}N_{12}O_6$: 850.46, found 851.34; Purity determined by RP-HPLC: Retention time: 24.231 min, purity: 98.74%.

4.4.22. H-Trp-Orn-Trp-3ABA-Trp-Orn-NH₂ **(4l):** ^{1}H NMR (400 MHz, DMSO d_6) δ: 10.98 (s, 3H), 10.87 (s, 1H), 10.82 (s, 1H), 10. 30 (s, 1H), 9.59 (s, 3H), 8.86 (s, 5H), 8.44 - 8.38 (d, *J* = 24Hz, 2H), 7.65 - 7.26 (m, 8H), 7.02 - 6.83 (m, 11H), 4.72 - 4.68 (m, 3H), 4.45 - 4.22 (m, 2H), 3.21 - 3.17 (d, *J* = 16Hz, 6H), 2.84 - 264 (m, 5H), 2.47 - 2.45 (m, 2H), 1.71 - 1.54 (m, 6H), 1.23 - 1.06 (m, 4H). MALDI-TOF: calcd for $C_{50}H_{58}N_{12}O_6$: 922.46, found 923.29; Purity determined by RP-HPLC: Retention time: 25.378 min, purity: 99.66%.

4.4.23. H-Arg-Arg-Phe-3ABA-Phe-Arg-NH₂ **(4m):** ^{1}H NMR (400 MHz, DMSO d_6) δ: 10.90 (s, 2H), 10.82 (s, 3H), 10. 77 (s, 3H), 10.35 (s, 6H), 9.39 (s, 2H), 8.51 (s, 2H), 7.58 - 7.56 (d, *J* = 8Hz, 2H), 7.49 - 7.02 (m, 13H), 4.61 - 4.54 (m, 3H), 4.17 - 4.16 (t, *J* = 4Hz, 2H), 3.11 - 3.10 (d, *J* = 4Hz, 6H), 2.83 (s, 3H), 2.47 - 2.45 (m, 6H), 1.24 - 1.07 (m, 13H). MALDI-TOF: calcd for $C_{43}H_{62}N_{16}O_6$: 898.5, found 899.39; Purity determined by RP-HPLC: Retention time: 24.871 min, purity: 98.21%.

4.4.24. H-Phe-Arg-Phe-3ABA-Phe-Arg-NH₂ **(4n):** ^{1}H NMR (400 MHz, DMSO d_6) δ: 10.89 (s, 2H), 10.80 (s, 3H), 10. 76 (s, 2H), 10.36 (s, 4H), 9.38 (s, 2H), 8.52 (s, 2H), 7.58 - 7.57 (d, *J* = 4Hz, 2H), 7.52 - 7.21 (m, 11H), 7.14 - 6.98 (m, 8H), 4.60 - 4.54 (m, 3H), 4.17 - 4.15 (t, *J* = 8Hz, 2H), 3.11 - 3.9 (d, *J* = 8Hz, 7H), 2.84 (s, 2H), 2.48 - 2.45 (m, 5H), 1.25 - 1.07 (m, 9H). MALDI-TOF: calcd for $C_{46}H_{59}N_{13}O_6$: 889.47, found 890.33; Purity determined by RP-HPLC: Retention time: 26.225 min, purity: 98.34%.

4.4.25. H-Orn-Orn-Phe-3ABA-Phe-Orn-NH₂ **(4o):** ^{1}H NMR (400 MHz, DMSO d_6) δ: 10.90 (s, 2H), 10.83 (s, 3H), 10.36 (s, 6H), 9.41 (s, 2H), 8.50 (s, 2H), 7.58 - 7.56 (d, *J* = 8Hz, 2H), 7.50 - 7.02 (m, 14H), 4.61 - 4.54 (m, 3H), 4.17 - 4.15 (t, *J* = 8Hz, 2H), 3.12 - 3.10 (d, *J* = 8Hz, 5H), 2.47 - 2.45 (m, 6H), 1.24 - 1.07 (m, 14H). MALDI-TOF: calcd for $C_{40}H_{56}N_{10}O_6$:

772.44, found 773.46; Purity determined by RP-HPLC: Retention time: 23.313 min, purity: 96.67%.

4.4.26. H-Phe-Orn-Phe-3ABA-Phe-Orn-NH_2 **(4p):** ^{1}H NMR (400 MHz, DMSO d_6) δ: 10.89 (s, 2H), 10.80 (s, 3H), 10.36 (s, 4H), 9.36 (s, 2H), 8.50 (s, 2H), 7.58 - 7.57 (d, *J* = 4Hz, 2H), 7.53 - 7.20 (m, 10H), 7.16 - 6.98 (m, 8H), 4.60 - 4.54 (m, 3H), 4.17 - 4.15 (t, *J* = 8Hz, 2H), 3.11 - 3.9 (d, *J* = 8Hz, 7H), 2.48 - 2.45 (m, 5H), 1.25 - 1.07 (m, 9H). MALDI-TOF: calcd for $C_{44}H_{55}N_9O_6$: 805.43, found 806.36; Purity determined by RP-HPLC: Retention time: 25.038 min, purity: 98.28%.

4.5. Antibacterial activity

The antibacterial activity of synthesized peptidomimetic molecules was determined by screening against a range of susceptible as well as drug resistant strains includes *Escherichia coli* (MTCC 723), *Pseudomonas aeruginosa* (MTCC 2295), *Staphylococcus aureus* (MTCC 3160), *Basilus subtilis* (MTCC 2763), and methicillin-resistant bacterial strains MRSA (ATCC BAA-1720) & MRSE (ATCC 51625). Drug resistant bacterial strains used in the present study were collected from Medicos laboratories, Chandigarh, India. Antibacterial susceptibility testing was carried out using a modification of the Clinical Laboratory Standard Institute (CLSI) micro dilution broth assay [41]. The assay was performed in sterile 96-well, flat-bottom polypropylene microtiter plates (SIGMA). Briefly, each well of 96-well plate was inoculated with 90 μL of approximately 2×10^5 CFU/mL of bacterial suspension per mL of Mueller-Hinton broth (HIMEDIA). Then 10 μL of serially diluted peptidomimetics over concentration ranging from 0.7-100 μg/mL was added to the wells of microtiter plate. The microtiter plates were incubated overnight with agitation at 37 °C and absorbance was read at 600 nm after 18 h. Cultures (approximately 2×10^5 CFU/ mL) without peptidomimetics were used as positive control. Uninoculated Mueller-Hinton broth was used as negative control. The tests were carried out in triplicate. The minimum inhibitory concentration (MIC) is defined as the lowest concentration of peptide that completely inhibits growth.

To analyze the dynamic behavior of the peptidomimetic molecules (**4g**, **4l**, **5b**, & **5d**) we performed molecular dynamic (MD) simulation by using UCSF CHIMERA version 1.4 (build 29530) on operating system win32. We carried out molecular mechanics operation in aqueous environment. We have chosen the initial coordinates of the molecules and calculated the energy by using conjugate gradient energy minimizer and perform a simulation. To minimize the structure we predicted several starting points in energy landscape and the optimal structure was one with lowest energy. Our experiment generated approximately 250 to 270 conformers for each molecule and after removal of duplicated minima; only conformations within 3.2 kcal/mol of the global minimum were considered. Finally, we have validated most stable structure for each molecule through Structure Analysis and Verification Server (SAVS).

4.7. Hemolytic assay

Hemolytic activity of the peptides was determined using fresh isolated hRBCs. The hRBCs were centrifuged for 15 min to remove the buffy coat and washed three times with phosphate buffer saline (35 mM phosphate buffer, 150 mM NaCl pH 7.2). 100 μL of the hRBC suspended 4% (v/v) in PBS was plated into sterilized 96-well plates and then 100 µL peptide solution (serial twofold dilution in PBS) was added to each well. The plates were incubated for 1 h at 37 °C without agitation and centrifuged at 1000 g for 5 min. Aliquots (100 µL) of the supernatant were transferred to 96-well plates, where hemoglobin release was monitored using microtiter plate reader (Bio-Rad, India) by measuring the absorbance at 540 nm. Percent hemolysis was calculated by the following formula:

$$\%\text{age hemolysis} = 100 \times [(A - A_0)/(A_t - A_0)]$$

Where, A represents absorbance of peptide sample at 540 nm and A_0 and A_t represent zero percent and 100% hemolysis determined in PBS and 1% Triton X-100, respectively.

4.8. Cell culture and cytotoxicity

HaCaT cells (Human keratinocytes) were obtained from National Centre for Cancer Science (NCCS), Pune and grown as a monolayer in DMEM supplemented with 10% FBS (Fetal Bovine Serum), 100 µg/mL streptomycin and 100 units/mL penicillin. Cells were incubated at 37 °C in an atmosphere of 5% CO_2.

4.8.1. MTT assay

The cell viability of HaCaT cells was assessed by the MTT colorimetric assay, which is based on the reduction of MTT by the mitochondrial succinate dehydrogenase of intact cells to a purple formazan product. Briefly, cells were incubated in 96-well microtiter plates for 24 h at 37 °C in a 5% CO_2 incubator. Following the addition of the test peptidomimetics, the plates were incubated for an additional 24 h. Control wells contained medium alone. Three replicate wells were used at each point in the experiments. After 24 h incubation, MTT solution (5 mg/mL in phosphate-buffered saline) was added and incubated for another 4 h. The resulting MTT/formazan product was dissolved by 100 µL of isopropanol and the plates were gently shaken to solubilise the formed formazan. The amount of formazan was determined by measuring the absorbance (OD) at 570 nm using a Bio-Rad 550 enzyme-linked immunosorbent assay (ELISA) microplate reader [42].

Cell survival was calculated as the percentage MTT inhibition as follows:

% growth inhibition = 100 − (mean OD of individual test group/ mean OD of each control group) ×100.

4.8.2. LDH assay

In LDH assay, leakage of the cytoplasmic located enzyme LDH into the extracellular medium is measured. Briefly, cells were incubated in 96-well microtiter plates for 24 h at 37 °C in a 5% CO_2 incubator. At 24 h after cell seeding, cells were exposed to varying concentrations of the test peptidomimetics. After 24 h of treatment, the supernatants were collected from each well. Cell monolayers were trypsinized and the cells and lysate were collected. LDH activity was measured in both the supernatants and the cell lysate fractions using Cyto-Tox 96, a non-

radioactive cytotoxicity assay kit, in accordance with the manufacturer's instruction. The intensity of color is proportional to LDH activity. LDH release was calculated by measuring the absorbance at 490 nm using ELISA microplate reader [43]. The percentage LDH release from the cells was determined using the following formula:

% LDH release = ((absorbance of the supernatant)/ absorbance of the supernatant and cell lysate)) ×100

4.9. Bactericidal kinetics

The time course of bacterial killing was studied by the exposure of *S. aureus* (MTCC 3160) and *E. coli* (MTCC 723) cultures (2×10^7 CFU/mL) to lead peptidomimetics (**4g** and **4l**) at 4 × MIC in Muller Hinton media. Aliquots were removed at a fixed time interval, diluted up to 10^8, plated on the Muller Hinton agar plate and CFU were counted after 24 h incubation at 37 °C. Untreated bacterial culture was used as a control. Data were obtained from two independent experiments performed in triplicate.

4.10. Membrane interaction study using membrane models

4.10.1. Preparation of calcein encapsulated liposomes

Large unilamellar vesicles (LUVs) of dipalmitoylphosphatidylcholine (DPPC) and dipalmitoylphosphatidylglycerol (DPPG) were prepared to mimic bacterial membrane (DPPC:DPPG, 7:3, w/w) or mammalian membrane (DPPC/ Chol, 10:1, w/w) as described previously [44]. Briefly, a defined amount of lipid mixture DPPC:DPPG (7:3) was dissolved in 2 mL chloroform/methanol solvent mixture in a 100 mL round bottom flask. The solvents were removed under a stream of nitrogen and the lipid film obtained was lyophilized overnight to remove any trace of solvent. The thin lipid film was rehydrated with calcein containing buffer comprising 70 mM calcein, 150 mM NaCl, and 0.1 mM EDTA and adjusted to pH 7.4 by the addition of a few drops of sodium hydroxide solution (1 M). The liposome suspension obtained after rehydration was frozen and thawed for five cycles and extruded 15 times through two stacked polycarbonate filters (100 nm pore size). The free

calcein was removed by passing the liposome suspension through a Sephadex G-50 column and eluting with a buffer containing 10 mM Tris-HCl (150 mM NaCl, 0.1 mM EDTA). After passing the liposome through Sephadex G-50, liposome diameter was measured by dynamic light scattering using a Zetasizer Nano ZS (Malvern Instruments, India). Average diameter of LUVs was found to be in the range of 110-130 nm.

4.10.2. Calcein dye leakage assay

Peptidomimetic induced leakage of calcein from the LUVs was monitored by measuring the fluorescence intensity at an excitation wavelength of 490 nm and an emission wavelength of 520 nm on a Fluoromax 4 (spex) spectrofluorometer. Aliquots of liposome suspension were then diluted in calcein free buffer (150 mM NaCl, 0.1 mM EDTA) to a final concentration of 40 μM lipid and incubated for 5 min with different concentrations of peptidomimetics (5-15 μg/mL). Calcein release from LUVs was assessed every minute for the first 20 min of the experiment and after onward measurement was taken at the interval of 10 min. The fluorescence intensity corresponding to 100% calcein release was determined by the addition of a 10% solution (w/v) of Triton X-100. The apparent percentage of dye leakage was calculated using the following formula:

$$\% \text{ Dye leakage} = 100 \times [(F - F_0)/ (F_t - F_0)]$$

Where F is the intensity measured at a given concentration of peptidomimetic, F_0 is the intensity of the liposomes (background), and F_t is the intensity after lysis by Triton X-100.

4.11. Fluorescence microscopy

In order to shed light on bactericidal mechanism of newly designed peptidomimetics fluorescence microscopy assay with DAPI (4’,6-Diamidino-2-phenylindole dihydrochloride, Sigma) and PI (Propidium iodide, Sigma) as fluorophores was performed by treating *E. coli* and *S. aureus* cells. In this double staining method we can easily visualize and differentiate viable cells from the dead cells. DAPI as a double stranded DNA binding dye, stains all bacterial cells irrespective of their viability. Whereas PI is capable of passing through only

damaged cell membranes and intercalates with the nucleic acids of injured and dead cells to form a bright red fluorescent complex. The cells were first stained with DAPI and then with PI. Bacterial cells were grown until they reached mid-logarithmic phase (2×10^6 cells) and then they were incubated with the peptidomimetics at the concentration of 4 × MIC for 2 h. Then the cells were pelleted by centrifugation at 3000g for 15 min in an eppendorf microcentrifuge. The supernatant was then decanted and the cells were washed with PBS several times and then incubated with PI (5 μg/mL) in the dark for 15 min at 0^oC. The excess PI was removed by washing the cells with PBS several times. Then the cells were incubated with DAPI (10 μg/mL) for 15 mins in dark at 0^oC. The DAPI solution was removed and cells were washed with PBS several times. Controls were performed following the exact same procedure for bacteria without the treatment with peptidomimetics. The bacterial cells were then examined by using the Nikon eclipse T*i* microscope with an oil-immersion objective (60×).

4.12. Resistance study

We determine the potential of susceptible as well as methicillin resistant *S. aureus* to develop antimicrobial resistance with our most potent peptidomimetic sequences **4g** and **4l**. The initial MIC values of lead peptidomimetics (**4g** and **4l)** and standard antibiotic ciprofloxacin against both bacterial strains was obtained as described above. Serial passage and MICs determination were performed in 96 well microtiter plate containing peptidomimetics, each over a range of doubling dilution concentrations. After the incubation period 18 h the entire content of the triplicate wells with a concentration of peptidomimetics permitting visible growth were then used to prepare the bacterial dilution (approximately 2×10^6 CFU/mL) for the successive exposure. The experiment was repeated for 16 days. As a positive control, parallel cultures were exposed to two fold dilutions of the standard antibiotic (ciprofloxacin).

4.13. Plasma stability study

In vitro stability study of representative peptidomimetics (**4g** and **4l**) and linear peptide sequences (**5b** & **5d**) were performed by using RP-HPLC as described previously [4]. A stock solution of peptidomimetics (1 mg/mL) was made by dissolving in water. Freshly collected heparinized blood plasma (1 mL) was added with 50 µL of peptidomimetic stock solution and incubated at 37 °C. Dilution of the human plasma was made in such a way that renders the proteolytic enzymes the limiting factor; enable a linear degradation of the peptidomimetics. After different time intervals (30 min, 1 h, 2 h, 6 h, 12 h, 24 h) 100 µL of the reaction solution was removed and added to 200 µL of 95% ethanol for precipitation of plasma proteins. The cloudy reaction sample is cooled at 4 ºC for 15 min and then centrifuge (18,000 g) for 2 min to pellet the precipitated proteins. The clear supernatant was then analyzed using RP-HPLC on a 5µm, 20 mm × 250 mm, Spherisorb® C-18 column with UV detection at 280 nm.

4.14. Proteolytic digestion assay

The stability testing of lead peptidomimetics (**4g** and **4l**) and linear peptide sequences (**5b** and **5d**) against trypsin and α-chymotrypsin was conducted using a modified version of earlier reported protocol [7]. Briefly, each test sample was dissolved in a 0.1 M NH_4HCO_3 buffer (pH 8.2) to a final concentration of 1 mg/mL. The enzymes (trypsin and α-chymotrypsin) solutions were prepared by dissolving 1 mg of enzyme to 50 mL of 0.1 M NH_4HCO_3 buffer (pH 8.2). The test sample solution (150 µL), enzyme solution (150 µL), and 0.1 M NH_4HCO_3 buffer (1200 µL) were combined and incubated at 37 ºC. Samples of 15 µL were collected at different time intervals, and 100 µL 10% (v/v) formic acid was added to stop the enzyme activity. For every test, a negative control without enzyme was incubated to ensure that whether the degradation was due to the enzyme or other factors. Quantitative analyses of the remaining amount of the test samples (**4g**, **4l**, **5b**, and **5d**) were performed by using RP-HPLC using a C_{18} waters column (Spherisorb®, ODS2, 5µm, 4.6 mm × 250 mm) at room temperature. Solvents used in this system were: Solvent A, purified water with 0.05% TFA,

and solvent B, HPLC grade acetonitrile with 0.05% TFA. The gradient chosen for separation started with an isocratic elution with 95% A and 5% B for 2 min, then a linear gradient to 40% A and 60% B after 3 min. The gradient was increased linearly to 10% A and 90% B after 10 min and was kept isocratic for 2 min. Flow speed was maintained at 0.2 mL/min for all set of experiments.

Acknowledgments

GSB thanks Department of science and Technology for financial support (SR/FT/CS-61/2010). We acknowledge Medicos laboratories, Chandigarh, India for providing drug resistant bacterial strains. We also acknowledge the Sophisticated Analytical Instrumentation Facility (SAIF), Punjab University, Chandigarh, India for providing the NMR facility.

References

[1]. S. Choi, A. Isaacs, D. Clements, D. Liu, H. Kim, R.W. Scott, J.D. Winkler, W.F DeGrado, De novo design and *in vivo* activity of conformationally restrained antimicrobial arylamide foldamers, Proc. Natl Acad. USA 106 (2009) 6968-6973.

[2]. G.N. Tew, R.W. Scott, M.L. Klein, W.F. Degrado, De novo design of antimicrobial polymers, foldamers, and small molecules: from discovery to practical applications, Acc. Chem. Res. 43 (2009) 30-39.

[3]. R.W. Scott, W.F. DeGrado, G.N. Tew, De novo designed synthetic mimics of antimicrobial peptides, Curr. Opin. Biotechnol. 19 (2008) 620-627.

[4]. B.E. Haug, W. Stensen, M. Kalaaji, Y. Rekdal, J.S. Svendsen, Synthetic antimicrobial peptidomimetics with therapeutic potential. J. Med. Chem. 51 (2008) 4306-4314.

[5]. B.E. Haug, W.Stensen, T. Stiberg, J. S. Svendsen, Bulky nonproteinogenic amino acids permit the design of very small and effective cationic antibacterial peptides, J. Med. Chem. 47 (2004**)** 4159-4162.

[6]. J. Svenson, W. Stensen, B.O. Brandsdal, B.E. Haug, J. Monrad, J.S. Svendsen, Antimicrobial peptides with stability toward tryptic degradation, Biochemistry 47 (2008) 3777-3788.

[7]. R. Karstad, G. Isaksen, B.O. Brandsdal, J. S. Svendsen, J. Svenson, Unnatural amino acid side chains as S1, S1', and S2' probes yield cationic antimicrobial peptides with stability toward chymotryptic degradation, J. Med. Chem. 53 (2010) 5558-5566.

[8]. M.B. Strøm, B.E. Haug, M.L. Skar, W. Stensen, T. Stiberg, J.S. Svendsen, The pharmacophore of short cationic antibacterial peptides, J. Med. Chem. 46 (2003) 1567-1570.

[9]. M. Zasloff, Antimicrobial peptides of multicellular organisms, Nature 415 (2002) 389-395.

[10]. A.T. Yeung, S.L. Gellatly, R.E. Hancock, Multifunctional cationic host defence peptides and their clinical applications, Cell. Mol. Life Sci. 68 (2011) 2161-2176.

[11] M.L. Mangoni, A. Carotenuto, L. Auriemma, M.R. Saviello, P. Campiglia, I. Gomez-Monterrey, S. Malfi, L. Marcellini, D. Barra, E. Novellino, P. Grieco Structure-activity relationship, conformational and biological studies of temporin L analogues, J. Med. Chem. *54* (2011**)** 1298-1307.

[12] T. Kiyota, S. Lee, G. Sugihara, Design and synthesis of amphiphilic alpha-helical model peptides with systematically varied hydrophobic-hydrophilic balance and their interaction with lipid- and bio-membranes, Biochemistry 35 (1996) 13196-13204.

[13] S.Y. Wei, J.M. Wu, Y.Y. Kuo, H.L. Chen, B.S. Yip, S.R. Tzeng, J.W. Cheng, Solution structure of a novel tryptophan-rich peptide with bidirectional antimicrobial activity, J. Bacteriol. 188 (2006) 328-334.

[14] R.E.W. Hancock, R. Lehrer, Cationic peptides: a new source of antibiotics, Trends Biotechnol. 16 (1998) 82-88.

[15] A. Giuliani, G. Pirri, S.F. Nicoletto, Antimicrobial peptides: an overview of a promising class of therapeutics, Cent. Eur. J. Biol. 2 (2007) 1-33.

[16] K.A. Brogden, M. Ackermann, P.B. McCray, B.F. Tack, Antimicrobial peptides in animals and their role in host defences, Int. J. Antimicrob Agents 22 (2003) 465-478.

[17] L. Zhang, P. Dhillon, H. Yan, S. Farmer, R.E. Hancock, Interactions of bacterial cationic peptide antibiotics with outer and cytoplasmic membranes of *Pseudomonas aeruginosa*, Antimicrob. Agents Chemother. 44 (2000) 3317-3321.

[18] M. Wu, E. Maier, R. Benz, R.E.W. Hancock, Mechanism of interaction of different classes of cationic antimicrobial peptides with planar bilayers and with the cytoplasmic membrane of *Escherichia coli*, Biochemistry 38 (1999) 7235-7242.

[19] Y. Shai, Z. Oren, From "carpet" mechanism to de-novo designed diastereomeric cell-selective antimicrobial peptides, Peptides 22 (2001) 1629-1641.

[20] J.M. Sanderson, Peptide-lipids interactions: insights and perspectives, Org. Biomol. Chem. 3 (2005) 201-212.

[21] L. Yang, T. Harroun, T.M. Weiss, L. Ding, H.W. Huang, Barrel-stave model or toroidal model? A case study on melittin pores, Biophys J. 811 (2001) 475-1485.

[22] L. Beven, O. Helluin, G. Molle, H. Duclohier, H. Wroblewski, Correlation between anti-bacterial activity and pore sizes of two classes of voltage dependent channel-forming peptides, Biochim. Biophys. Acta 1421 (1999) 53-63.

[23] L. Yang, T.M. Weiss, R.I. Lehrer, H.W. Huang, Crystallization of antimicrobial pores in membranes: magainin and protegrin, Biophys J. 79 (2001) 2002-2009.

[24] M.L. Mangoni, Host-defense peptides: from biology to therapeutic strategies, Cell. Mol. Life Sci. 68 (2011) 2157-2159.

[25] W.C. Wimley, Describing the mechanism of antimicrobial peptide action with the interfacial activity model, ACS Chem. Biol. 5 (2010) 905-917.

[26]. B. Findlay, G.G. Zhanel, F. Schweizer, Cationic amphiphiles, a new generation of antimicrobials inspired by the natural antimicrobial peptide scaffold, Antimicrob. Agents Chemother. 54 (2010) 4049-4058.

[27]. M.A. Schmitt, B. Weisblum, S.H. Gellman, Interplay among folding, sequence, and lipophilicity in the antibacterial and hemolytic activities of α/*β*-Peptides, J. Am. Chem. Soc. 129 (2007) 417-428.

[28]. G. Srinivasulu, M.H.V. Ramana Rao, S. Kiran Kumar, A.C. Kunwar, β-Hairpin peptides containing 3-amino benzoic acid, a constrained γ-amino acid, Arkivoc (2004) 69-86.

[29]. M.H.V. Ramana Rao, S. Kiran Kumar, A.C. Kunwar, Formation of β-hairpins in L-Pro-Gly containing peptides facilitated by 3-amino benzoic acid, Tetrahedron Lett. 44 (2003) 7369-7372.

[30]. F.T. Lundya, J. Nelson, D. Lockhart, B. Greer, P. Harriott, J.J. Marley, Antimicrobial activity of truncated α-defensin (human neutrophil peptide (HNP)-1) analogues without disulphide bridges, Mol. Immunol. 45 (2008) 190-193.

[31]. G.A. Lengyel, G.A. Eddinger, W.S. Horne. Introduction of cyclically constrained γ-residues stabilizes an α-peptide hairpin in aqueous solution, Org. Lett. 15 (2013) 944-947.

[32]. T. Hansen, T. Alst, M. Havelkova, M.B. Strøm, Antimicrobial activity of small *β*-peptidomimetics based on the pharmacophore model of short cationic antimicrobial peptides, J. Med. Chem. 53 (2010) 595-606.

[33]. S. Lohan, G.S. Bisht, Small cationic antimicrobial peptidomimetics: emerging candidate for the development of potential anti-infective agents, Curr. Pharm. Des. 19 (2013) 5809-5823.

[34]. A. Wessolowski, M. Bienert, M. Dathe, Antimicrobial activity of arginine- and tryptophan-rich hexapeptides: the effects of aromatic clusters, D-amino acid substitution and cyclization, J. Pept. Res. 64 (2004) 159-169.

[35]. L.H. Kondejewski, D.L. Lee, M. Jelokhani-Niaraki, S.W. Farmer, R.E.W. Hancock, R.S. Hodges, Optimization of microbial specificity in cyclic peptides by modulation of hydrophobicity within a defined structural framework, J. Biol. Chem. 277 (2002) 67-74.

[36]. C. Auvynet, Y. Rosenstein, Multifunctional host defense peptides: Antimicrobial peptides, the small yet big players in innate and adaptive immunity, FEBS J. 276 (2009) 6497-6508.

[37]. M. Ahn, R.N. Murugan, B. Jacob d, J.K. Hyun, C. Cheong, E. Hwang, H.N. Park, J.H. Seo, G. Srinivasrao, K.S. Lee, S.Y. Shin d, J.K. Bang, Discovery of novel histidine-derived lipo-amino acids: Applied in the synthesis of ultra-short antimicrobial peptidomimetics having potent antimicrobial activity, salt resistance and protease stability, Eur. J. Med. Chem. 68 (2013) 10-18.

[38]. R.N. Murugan, B. Jacob, E.H. Kim, M. Ahn, H. Sohn, J.H. Seo, C. Cheong, J.K. Hyun, K.S. Lee, S.Y. Shin b, J.K. Bang, Non hemolytic short peptidomimetics as a new class of potent and broad-spectrum antimicrobial agents, Bioorg. Med. Chem. Lett. 23 (2013) 4633-4636.

[39]. G.G. Perron, M. Zasloff, G. Bell, Experimental evolution of resistance to an antimicrobial peptide, Proc. Biol. Sci. 273 (2006) 251-256.

[40]. R.B. Merrifield, Solid phase synthesis, Science 232 (1986) 341-347.

[41]. M.A. Wikler, D.E. Low, F.R. Cockerill, D.J. Sheehan, W.A. Craig, F.C. Tenover, M.N. Dudley, Methods for dilution antimicrobial susceptibility tests for bacteria that grow aerobically: approved standard-seventh edition, CLSI (formerly NCCLS) (2006) M7-A7.

[42]. F. Denizot, R. Lang, Rapid colorimetric assay for cell growth and survival. Modifications to the tetrazolium dye procedure giving improved sensitivity and reliability, J. Immunol. Methods 89 (1986) 271-277.

[43]. R. A. Vaucher, M. L. Teixeira, A. Brandelli, Investigation of the cytotoxicity of antimicrobial peptide P40 on eukaryotic cells, Curr. Microbiol. 60 (2010) 1-5.

[44]. L. Zhang, A. Rozek, R.E.W. Hancock, Interaction of cationic antimicrobial peptides with model membranes, J. Biol. Chem. 276 (2001) 35714-35722.

Figure legends

Scheme 1. Overview of the solid phase synthesis of 3-ABA scaffold based cationic peptidomimetics. Reagents and reaction conditions (a) Deprotection; 20% piperidine. (b) Coupling; Fmoc-Arg(Pbf)-OH or Fmoc-Orn(Boc)-OH, HOBt, DIPC, DMF. Deprotection; 20% piperidine. (c) Coupling; Fmoc-3-ABA-OH, HOBt, DIPC, DMF. Deprotection; 20% piperidine. (d) Coupling; Fmoc-Trp(Boc)-OH, HOBt, DIPC, DMF. Deprotection; 20% piperidine. (e) Cleavage; TFA : 1, 2-Ethanedithiol : H_2O (95:2.5:2.5). (f) Coupling; Fmoc-Arg(Pbf)-OH or Fmoc-Trp(Boc)-OH, HOBt, DIPC, DMF. Deprotection; 20% piperidine. (g) Coupling; Fmoc-Arg(Pbf)-OH or Fmoc-Orn(Boc)-OH or Fmoc-Trp(Boc)-OH or Fmoc-Phen-OH, HOBt, DIPC, DMF. Deprotection; 20% piperidine. (h) Coupling; Fmoc-Arg(Pbf)-OH or Fmoc-Orn(Boc)-OH or Fmoc-Trp(Boc)-OH, HOBt, DIPC, DMF. Deprotection; 20% piperidine.

Figure 1: Structural overview of the small peptide sequence having 3-ABA as a peptidomimetic element with bond angles present in the structural framework of 3-ABA.

Figure 2: 3D structural view of the lowest energy conformers of lead peptidomimetics (**4g** and **4l**) and linear peptides (**5b** and **5d**). Structural optimization experiments were conducted by using UCSF CHIMERA version 1.4.

Figure 3: Chemical structure of active peptidomimetic sequences (**3e**, **4f**, **4g, 4k** and **4l**) having a hydrophobic core as common structural feature.

Figure 4: Concentration-dependent effect of lead peptidomimetics (**4g** & **4l**) and linear peptides (**5b** & **5d**) on cell viability of HaCaT cells determined by MTT assay. The results represent the data (mean ± SD) obtained from two independent experiments performed in triplicate.

Figure 5: LDH release from HaCaT cells treated with lead peptidomimetics (**4g** & **4l**) and linear peptides (**5b** & **5d**) at various concentrations. The results represent the data (mean ± SD) obtained from two independent experiments performed in triplicate.

Figure 6: Bactericidal kinetics of lead cationic peptidomimetics **4g** and **4l** at 4 × MIC. (A) against *S. aureus*. (B) against *E. coli*. The data obtained are from two independent experiments performed in triplicate.

Figure 7: Concentration-dependent leakage of calcein dye from negatively charged [DPPC/DPPG (7:3, w/w)] LUVs measured after 5 min of incubation of cationic peptidomimetics **4g** (A) and **4l** (B) at different concentrations with LUVs.

Figure 8: Fluorescence micrographs of *E. coli* and *S. aureus* treated with **4g** and **4l** (4 × MIC) for 2 h: (A1-A6) *E. coli*; (A1) control, no treatment, DAPI stained; (A2) control, no treatment, PI stained; (A3) **4g** treatment, DAPI stained; (A4) **4g** treatment, PI stained; (A5) **4l** treatment, DAPI stained; (A6) **4l** treatment, PI stained. (B1-B6) *S. aureus*; (B1) control, no treatment, DAPI stained; (B2) control, no treatment, PI stained; (B3) **4g** treatment, DAPI stained; (B4) **4g** treatment, PI stained; (B5) **4l** treatment, DAPI stained; (B6) **4l** treatment, PI stained.

Figure 9: Evaluation of resistance development against lead peptidomimetics **4g** and **4l** in bacterial strains (A) *S. aureus* (MTCC 3160) and (B) Methicillin resistant *S. aureus* (MRSA, ATCC BBA-1720).

Figure 10: In vitro proteolytic digestion assay of lead peptidomimetics (**4g** and **4l**) and linear peptides (**5b** and **5d**) against trypsin (A) and α-chemotrypsin (B). Percentage of the remaining test sample was measured using analytical RP-HPLC.

Table 1: Antibacterial activity of small cationic peptidomimetics.

Code	Sequence[a]	MIC (μg/mL)						hemolysis[b]	selectivity[c]
		E.coli	*P.aeruginosa*	*S.aureus*	*B. subtilis*	MRSA	MRSE	HC_{10}/HC_{50}	
1a	W-3ABA-R-NH_2	>200	>200	>200	>200	>200	>200	400/>500	-
2a	WW-3ABA-R-NH_2	150	170	120	150	200	>200	100/240	2
2b	RW-3ABA-R-NH_2	70	75	50	100	60	70	205/500	10
2c	WR-3ABA-R-NH_2	200	>200	150	200	150	200	300/>500	>3.3
3a	WW-3ABA-RR-NH_2	120	125	50	70	50	75	150/400	8
3b	RW-3ABA-RR-NH_2	100	75	70	100	75	75	350/>500	>7.14
3c	WR-3ABA-RR-NH_2	>200	>200	100	170	120	100	325/>500	>5
3d	WR-3ABA-WR-NH_2	150	120	60	75	50	75	220/400	6.66
3e	RW-3ABA-WR-NH_2	40	50	12.5	50	10	12.5	250/410	32.8
4a	WWR-3ABA-RR-NH_2	75	100	50	70	50	50	200/380	7.6
4b	RWR-3ABA-WR-NH_2	120	120	50	125	40	50	210/400	8
4c	RWW-3ABA-RR-NH_2	70	75	25	75	25	25	255/420	16.8
4d	WRR-3ABA-WR-NH_2	50	50	15	70	12.5	10	190/380	25.33
4e	WRW-3ABA-RR-NH_2	60	70	25	40	25	25	140/370	14.8
4f	RRW-3ABA-WR-NH_2	17.5	25	6.25	25	5	6.25	100/355	56.8
4g	WRW-3ABA-WR-NH_2	7.5	12.5	5	20	5.5	5	80/310	62
3f	OW-3ABA-WO-NH_2	50	40	17.5	50	20	15	190/>500	>28.57
4h	OWW-3ABA-OO-NH_2	100	100	50	100	50	50	150/440	8.8
4i	WOO-3ABA-WO-NH_2	75	100	40	75	50	40	170/500	12.5
4j	WOW-3ABA-OO-NH_2	70	75	25	40	25	20	175/450	18
4k	OOW-3ABA-WO-NH_2	40	50	7.5	40	10.25	12.5	120/450	60
4l	WOW-3ABA-WO-NH_2	20	15.5	6.25	25	5	6.25	100/390	62.4
4m	RRF-3ABA-FR- NH_2	>200	>200	150	200	150	170	130/375	2.5
4n	FRF-3ABA-FR- NH_2	>200	>200	120	150	125	120	125/310	2.58

4o	OOF-3ABA-FO- NH_2	>200	>200	>200	>200	>200	>200	210/490	-
4p	FOF-3ABA-FO- NH_2	>200	>200	150	>200	>200	>200	180/400	2.66
5a	RRWWR-NH_2	75	100	25	70	25	20	90/240	9.6
5b	WRWWR-NH_2	40	70	15	50	17.5	20	60/200	13.33
5c	OOWWO-NH_2	120	150	70	100	100	100	100/310	4.42
5d	WOWWO-NH_2	70	150	50	120	50	70	65/225	4.5
	Ciprofloxacin	0.7	0.3	0.15	0.7	-	-	-	-
	Vancomycin	-	-	-	-	1.5	2	-	-

[a]Amino acids are represented by their one letter denotion.

[b]HC_{10} and HC_{50} are the concentrations in µg/mL of peptidomimetic molecule at which 10% or 50% hemolysis was observed.

[c]Selectivity is calculated based on HC_{50}/ MIC of *S. aureus*.

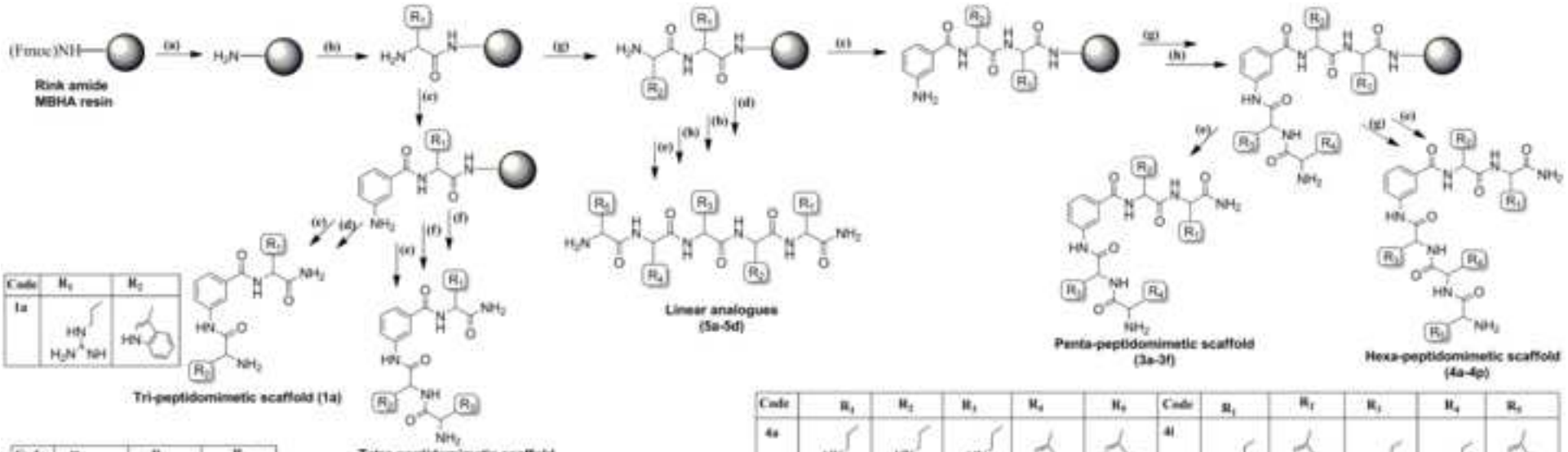

Code	R_1	R_2
1a		

Code	R_1	R_2	R_3
2a		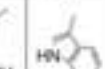	
2b			
2c			

Code	R_1	R_2	R_3	R_4
3a				
3b				
3c				
3d				
3e				
3f				

Code	R_1	R_2	R_3	R_4	R_5	Code	R_1	R_2	R_3	R_4	R_5
4a						4i					
4b						4j					
4c						4k 5c					
4d						4l 5d					
4e						4m					
4f 5a						4n					
4g 5b						4o					
4h						4p					

Figure(s)

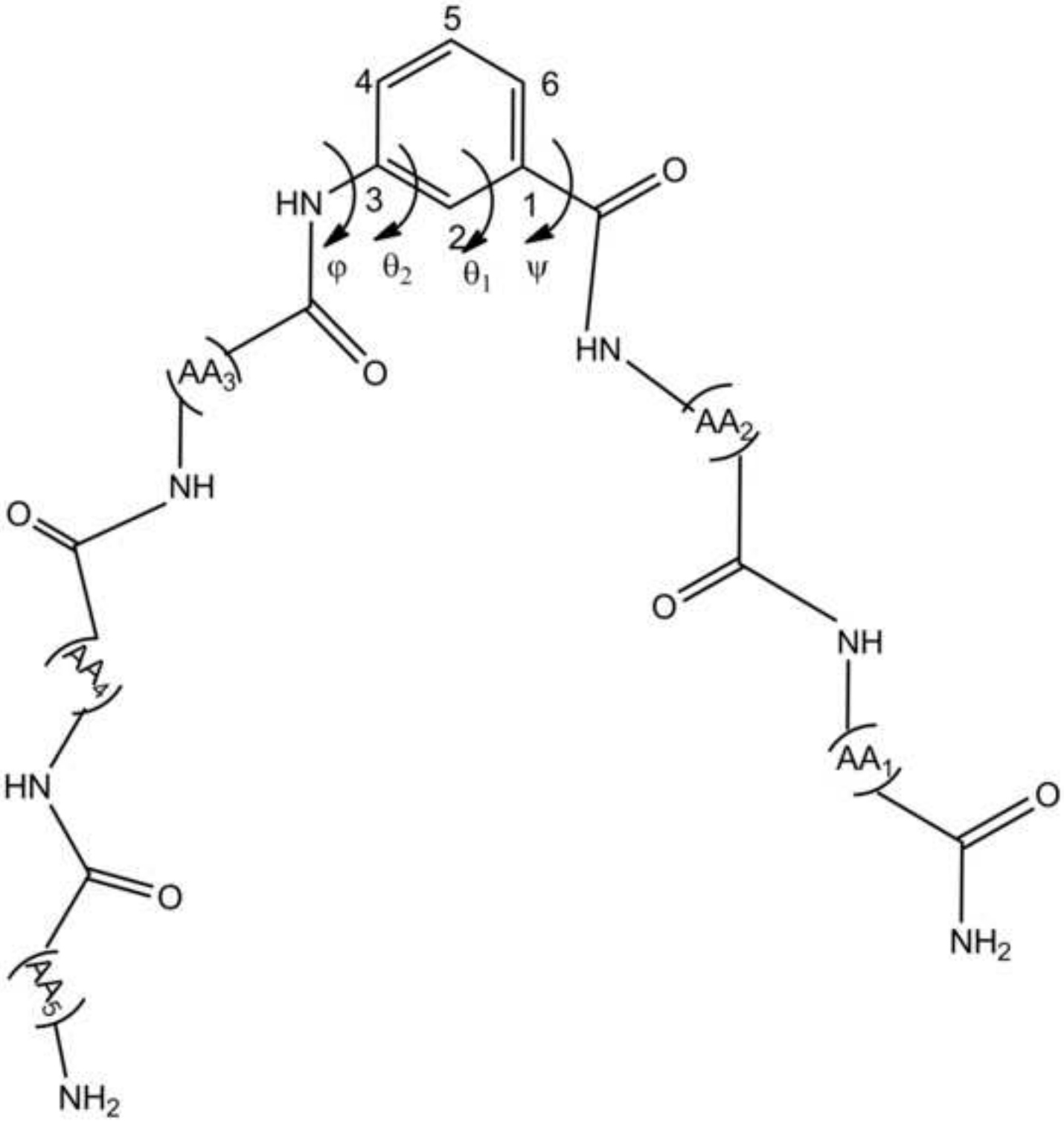

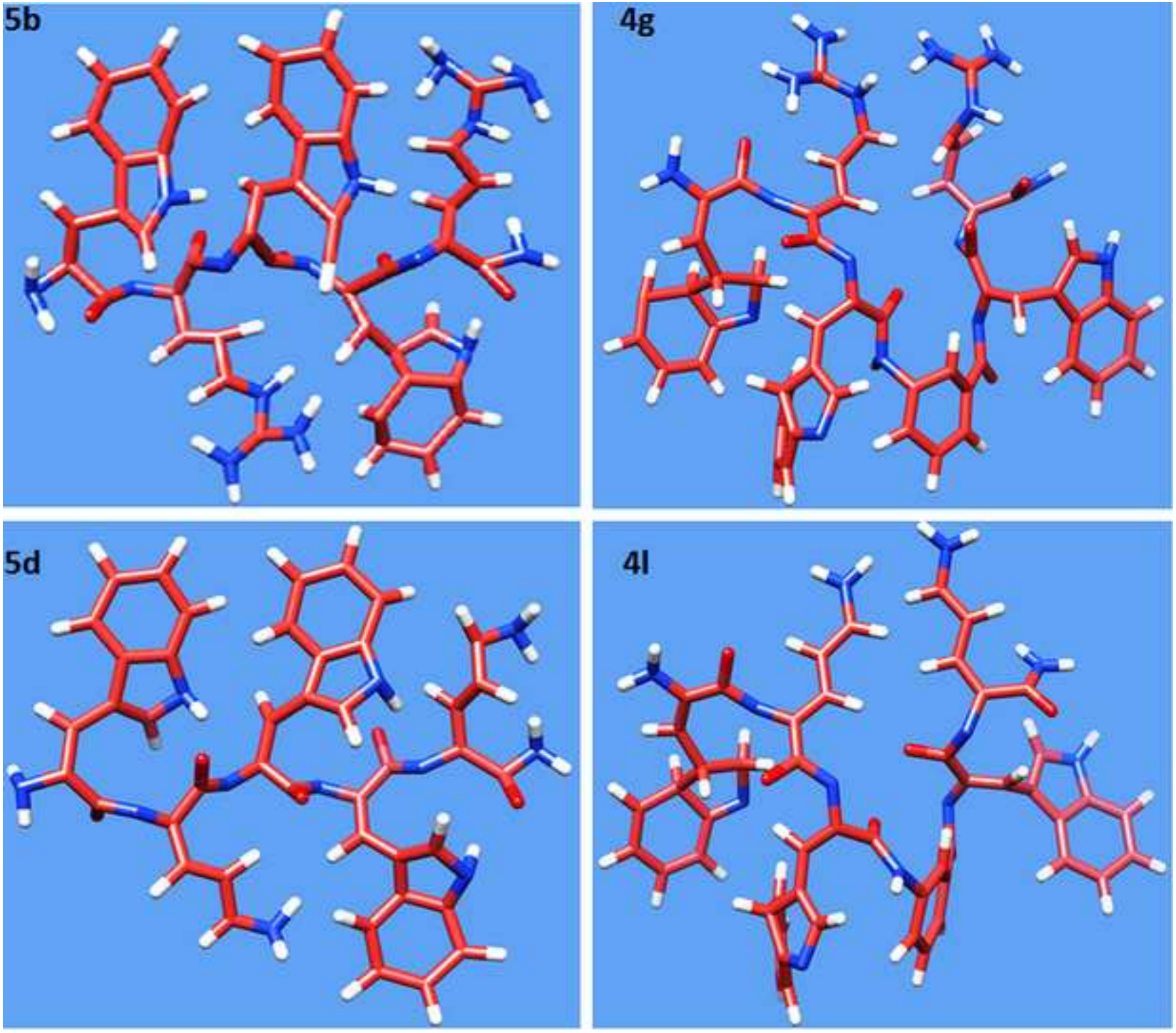

Peptidomimetic sequence (**3e**)

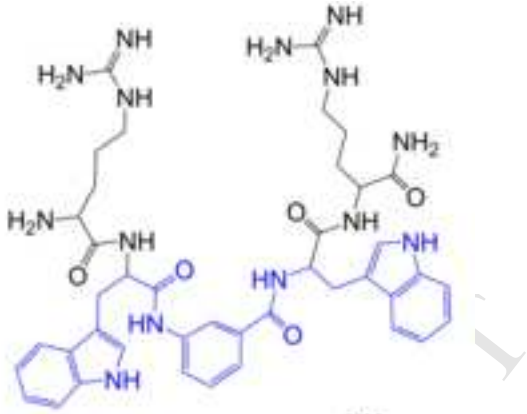

Peptidomimetic sequence (**4f**)

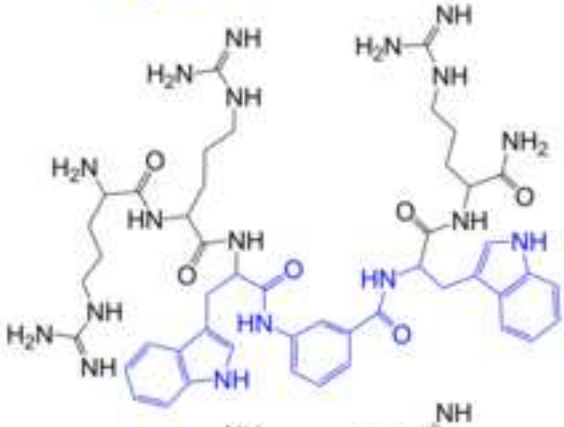

Peptidomimetic sequence (**4g**)

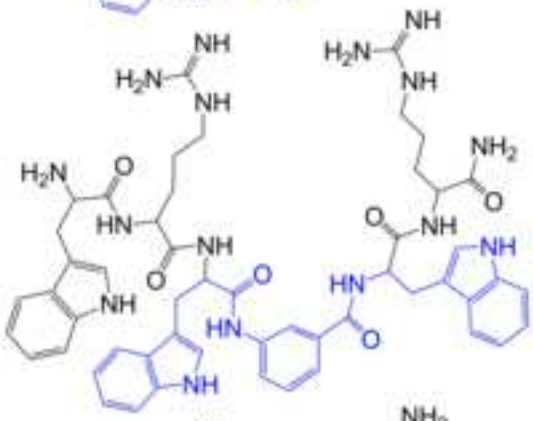

Peptidomimetic sequence (**4k**)

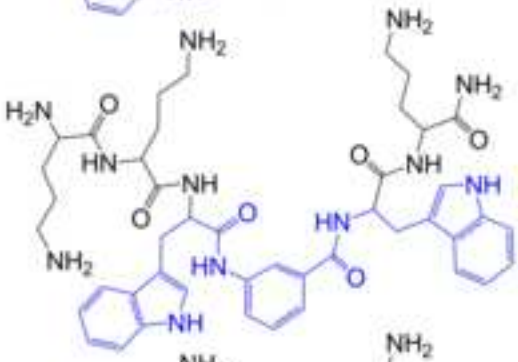

Peptidomimetic sequence (**4l**)

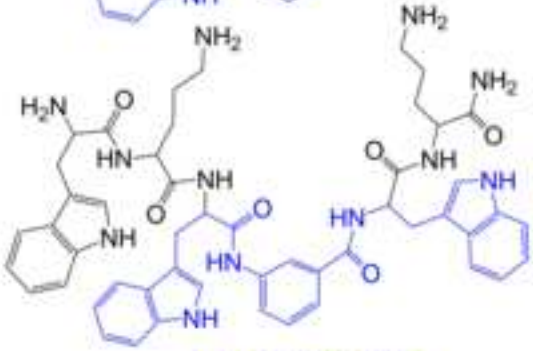

Hydrophobic core

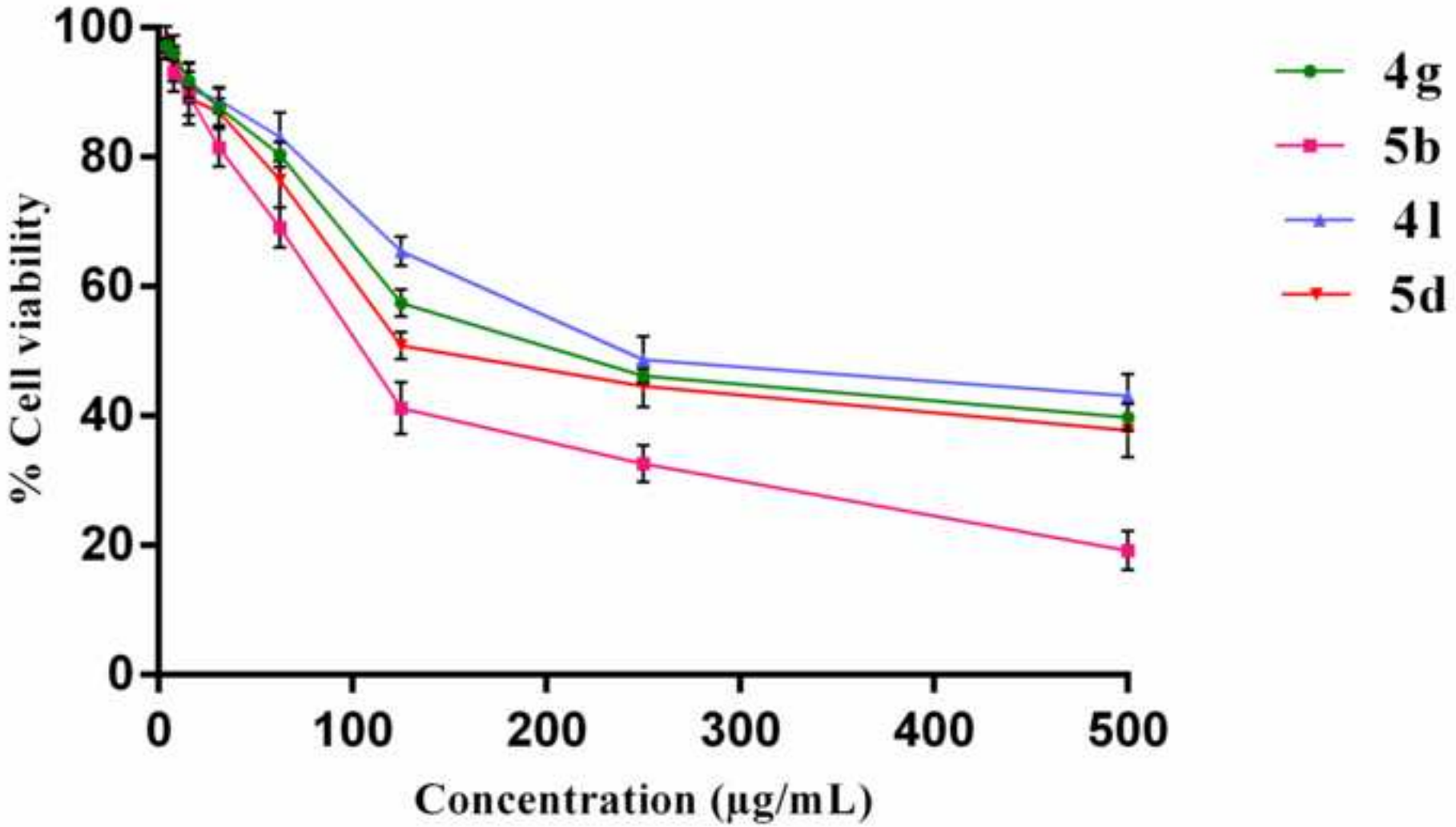

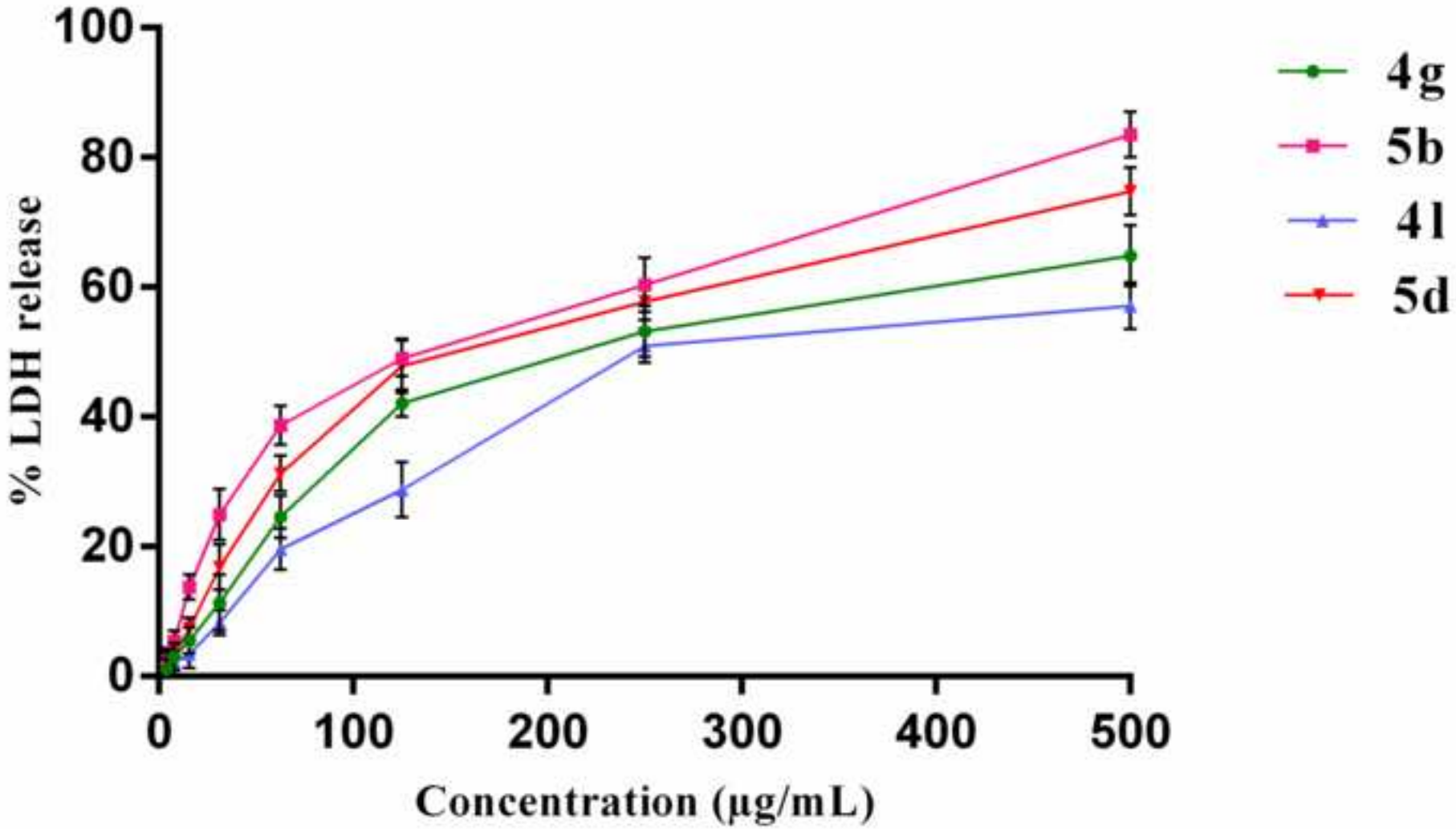

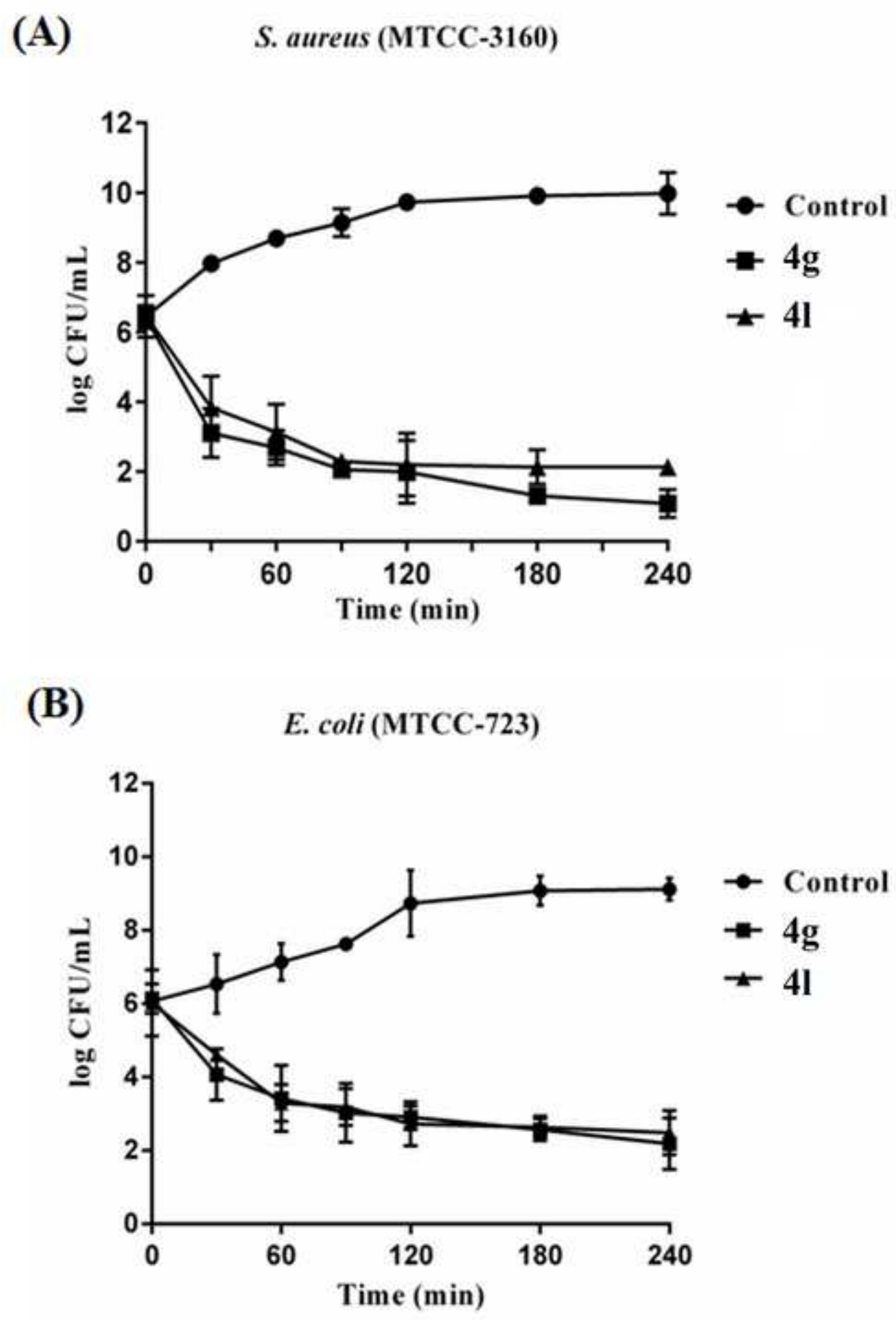

(A)

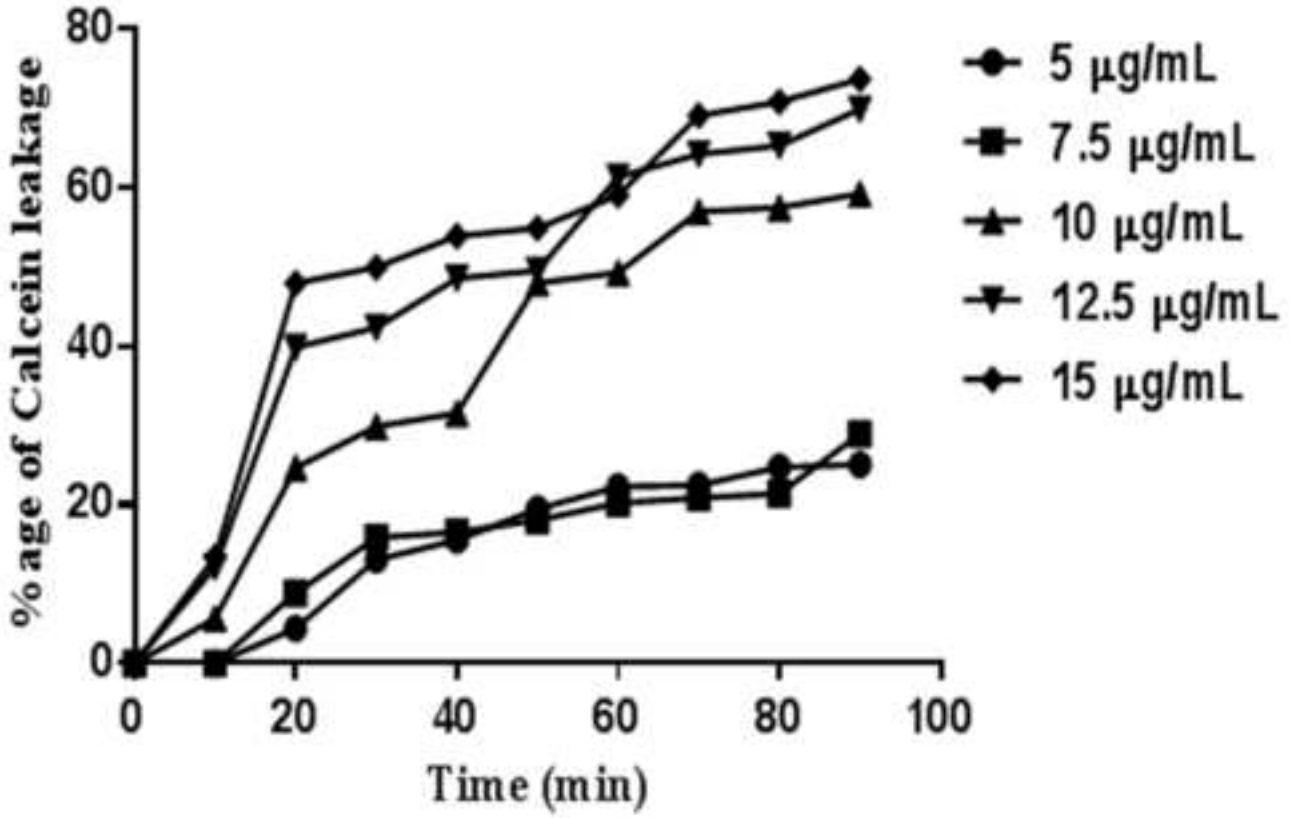

(B)